Ts1Cje Down syndrome model mice exhibit environmental stimuli-triggered locomotor hyperactivity and sociability concurrent with increased flux through central dopamine and serotonin metabolism

（ダウン症モデルマウス; Ts1Cje は、中枢ドーパミン、セロトニンの増加
並びにそれらの代謝亢進を示すと共に環境刺激誘発による
活動量と社会性の増加を示す）

２０１７年９月

埼玉大学大学院理工学研究科（博士後期課程）

理工学専攻　連携先端研究コース（主指導教員　山川 和弘）

下畑　充志

Ts1Cje Down syndrome model mice exhibit environmental stimuli-triggered locomotor hyperactivity and sociability concurrent with increased flux through central dopamine and serotonin metabolism

(ダウン症モデルマウス；Ts1Cje は、中枢ドーパミン、セロトニンの増加並びにそれらの代謝亢進を示すと共に環境刺激誘発による活動量と社会性の増加を示す)

2017 年 9 月

埼玉大学大学院理工学研究科（博士後期課程）

理工学専攻　連携先端研究コース

（主指導教員　山川　和弘）

下畑　充志

Summary

Down syndrome (DS) or trisomy 21 is the most common genetic cause of intellectual disability and is characterized by a myriad of phenotypes affecting various organs. Several mouse models of DS have been established and constitute useful tools for defining the etiology of DS. Ts1Cje mouse carrying a 7.6 Mb segmental trisomy of mouse chromosome 16 (MMU16) is among the most commonly used DS models. Ts1Cje mice display a subset of features that mimic human DS, notably craniofacial abnormalities and deficits in learning and memory. A number of molecular and physiological parameters are also affected in these mice, including oxidative stress increase and mitochondrial dysfunction, abnormal neuronal dendritic spines, abnormal synaptic plasticity, deficient embryonic and adult neurogenesis and enhanced cell proliferation in ganglionic eminences. Despite the occurrence of affective and emotional impairments in patients with Down syndrome, these parameters are poorly documented in Down syndrome mouse models, including Ts1Cje mice. Here, we developed a comprehensive approach using the Ts1Cje model in order to investigate eventual behavioral-molecular correlations. We designed and describe for the first time a large behavior screening focusing on spontaneous activity, social behavior, anxiety and depression-like behavior in various conditions. We coupled this study to a molecular study using both in-vivo microdialysis and tissue punch measurements of monoamines levels in brains from Ts1Cje mice. Ts1Cje mice were hyperactive and possibly less anxious compared to WT mice in novel environments, but significantly less active in familiar environments. Ts1Cje also showed increased social contacts with unfamiliar partners compared to their WT littermates in two different testing paradigms. Ts1Cje

mice also exhibited signs of decreased depression like-behavior. Furthermore, Ts1Cje mice showed motor coordination deficit. As locomotor hyperactivity is often associated with enhanced striatal dopaminergic neurotransmission, we measured extracellular and total content of monoamines. By using intracerebral microdialysis and tissue extracts of the striatum and ventral forebrain, we also provide evidence that extracellular dopamine (DA) and serotonin (5-HT) and their total amounts are increased in Ts1Cje mice. In addition, we found that biosynthesis and degradation of DA was accelerated in Ts1Cje striatum by using biochemical and immunohistochemical analyses. These changes in monoamines could underlie the abnormal affective and emotional behaviors observed in Ts1Cje mice. Using a comprehensive battery of behavioral tests, we identified environmental novelty stimuli-triggered hyperactivity, increased sociability, and decreased depression-like behavior in Ts1Cje mice. Our neurochemical and immunohistochemical results further suggested that Ts1Cje mice show an abnormal increase in DA and 5-HT combined with an enhanced metabolism of these transmitters, which may help explain the affective and emotional abnormalities. Especially, reports on DA metabolism in brain samples from DS patients have been rather controversial. In some cases reported in the literature, DA was decreased in the brains of elder DS patients but not in young adult with DS. The discrepancies in human studies may be due to age-specific changes and to the fact that samples were extracted post-mortem (after natural death). Although the monoamine concentration in brains from young adults with DS is still unclear, our results suggest that it is likely not decreased. Our study suggests that more extensive investigation should thus be considered before implementing monoamine treatments in DS. Monoamine metabolism alterations still

require further investigation in order to understand how they are involved in the developmental and functional deficits in the brains of DS patients. Finally, our finding contributes to the understanding of molecular pathology of DS and may inform development of effective therapeutic approaches (Shimohata et al., 2017).

Table of Contents

1. Introduction --7

2. Materials and methods -10

2.1. Animals and experimental conditions -10

2.2. General health and neurological screen -11

2.3. Open field test -11

2.4. Elevated plus maze test -11

2.5. 24-hours locomotor activity monitoring in the home cage -12

2.6. Social interaction in a novel environment -12

2.7. Three-chamber sociability test -12

2.8. Porsolt forced swim test -13

2.9. Light/Dark transition test -14

2.10. Motor function tests -14

2.11. Hot plate test -15

2.12. Startle response/prepulse inhibition -15

2.13. Tail suspension test -16

2.14. Data analysis -16

2.15. Microdialysis -17

2.16. Tissue Collection and Neurochemical Analysis -18

2.17. Immunohistochemistry -20

2.18. Western blot -20

3. Results -22

3.1. Ts1Cje mice show locomotor hyperactivity in unfamiliar environments -22

3.2. Ts1Cje mice show decreased activity in familiar environments -23

3.3. Ts1Cje mice show increased sociability in unfamiliar environments and with novel partners -23

3.4. Decreased depression-like behavior in Ts1Cje mice -25

3.5. Other behavioral abnormalities in Ts1Cje mice -26

3.6. Increased basal extracellular and total content of dopamine and serotonin in Ts1Cje mice -27

3.7. Increased levels of phenylalanine and tyrosine, monoamine turnover and abnormal expression of their catabolic enzymes in Ts1Cje mice -29

4. Discussion -31

5. Figure -38

6. Supplementary Figure -49

7. Table -60

8. Acknowledgments -64

9. References -65

1. Introduction

Down syndrome (DS), a complex disorder caused by an extra copy of human chromosome 21 (HSA21), is characterized by a myriad of phenotypes affecting various organs, among which intellectual disability and neurological abnormalities are remarkable for their high penetrance (Epstein, 2001). Since the distal end of chromosome 16 (MMU16) shows conserved synteny to a large portion of HSA21, multiple mouse models carrying segmental trisomy of MMU16 have been developed (see review by Das and Reeves, 2011). Ts(17^{16})65Dn (referred to as Ts65Dn) mice, the most intensively studied model to date, carry a 13.2 Mb segmental trisomy of MMU16 (Davisson et al., 1990). A second mouse model, Ts(16C-tel)1Cje (referred to as Ts1Cje), has a smaller segmental trisomy (7.6 Mb) from the same fragment of MMU16 (Sago et al., 1998). Ts2Cje mice have an equivalent trisomic segment to that of Ts65Dn mice (Villar et al., 2005). Ts1Rhr mice have a smaller trisomic segment (4.2 Mb) consisting of 33 genes (Olson et al., 2007). The comparative study of these partial trisomy models is helpful to explore the relationship between gene dosage and phenotype (Sago et al., 2000). We previously showed dose-dependent gene over-expression (Amano et al., 2004), increased oxidative stress, tau hyperphosphorylation, mitochondrial dysfunction (Shukkur et al., 2006) and increased cell proliferation in ganglionic eminences (Ishihara et al., 2014) in Ts1Cje mice. We also found enlarged ventricles, impaired embryonic and adult neurogenesis (Ishihara et al., 2010) and increased oxidative stress (Ishihara et al., 2009) in Ts1Cje and Ts2Cje mice. Moreover, we recently reported that the enlargement of brain ventricles in Down syndrome mice is caused by a *Pcp4* dose-dependent cilia dysfunction (Raveau et al., 2017). DS mouse models display DS-like phenotypes, including

notably craniofacial abnormalities (Richtsmeier et al., 2000; 2002) and learning and memory deficits and/or abnormal neuron morphology and function (Davisson et al., 1990; Sago et al., 1998; Siarey et al., 2005; Belichenko et al., 2007; Belichenko et al., 2009). Some of the deficits observed in Ts65Dn mice (such as spatial learning and memory) are conserved in the shorter Ts1Cje triplication (Reeves et al., 1995; Sago et al., 1998, 2000), whereas others, such as working memory-related tasks (both short- and long-term) are impaired only in Ts65Dn mice (Fernandez et al., 2007; Kleschevnikov et al., 2012). However, possibly conflicting results were reported in Ts1Cje mice depending on the task, with a deficit in the T-maze but not novel object recognition (Belichenko et al., 2007; Fernandez and Garner, 2007). Overall, learning and memory deficits are milder in Ts1Cje mice than Ts65Dn mice, but the triplicated fragment in Ts1Cje mice is thought to include critical gene(s) responsible for DS cognitive dysfunction (Sago et al., 2000). Ts1Rhr mice harboring an even smaller trisomic segment still show significant cognitive and synaptic neurobiological phenotypes (Belichenko et al., 2009).

Apart from cognitive impairment and developmental delay, children with DS are highly affectionate and sociable (Kasari et al., 1990). They show signs of hyperactivity in the form of reduced behavioral inhibition, surgency/positive affect, less sadness (Nygaard et al., 2002) and enhanced impulsivity (Pueschel et al., 1991). However, later in life DS patients tend to develop anxiety, depression and regression symptoms especially around early adulthood (Collacott et al., 1992; McCarthy and Boyd, 2001; Stein et al., 2013). Reported changes in locomotor activity are inconsistent across the different models: Ts65Dn mice show hyperactivity, whereas Ts1Cje mice are hypoactive, and reduced anxiety has been described only in Ts65Dn mice (Davisson et al., 1990; Coussons-Read and Crnic, 1996; Reeves et al., 1995). These behavioral characteristics remain poorly described in DS mouse models and

their molecular basis in DS in both human and mice remain unexplained.

Quantitative alterations to dopamine (DA), serotonin (5-HT) and noradrenaline (NA) neurotransmitters in the central nervous system play an important role in behavioral and emotional changes in humans and rodents (Roeper 2013; Hovatta and Barlow, 2008; McCall et al., 2015; Giros et al., 1996; Mosienko et al., 2012; Xu et al., 2000). Whereas the concentrations of these monoamines were found decreased in post-mortem extracted cerebral tissue from persons with DS (Yates et al., 1983; Reynolds and Godridge, 1985; Godridge et al., 1987; Risser et al., 1997; Seidl et al., 1999) they appeared increased in cerebrospinal fluid (CSF) from individuals with DS (Kay et al., 1987; Schapiro et al., 1987). Thus, although these neurochemical changes in DS are still under debate, alterations in neurochemical concentrations in brain and CSF may play a role in behavioral and emotional changes in individuals with DS. To date, there have been no reports determining the amounts and release of neurotransmitters in the brains of Ts1Cje mice.

In the present study, we developed a comprehensive approach using the Ts1Cje model in order to investigate eventual behavioral-molecular correlations. We designed and describe for the first time a large behavior screening focusing on spontaneous activity, social behavior, anxiety and depression-like behavior in various conditions. We coupled this study to a molecular study using both in-vivo microdialysis and tissue punch measurements of monoamines levels in brains from Ts1Cje mice (Shimohata et al., 2017).

2. Materials and methods

2.1. Animals and experimental conditions

Ts(16C-tel)1Cje, referred to as Ts1Cje were maintained by backcrossing Ts1Cje males with C57BL/6J females for more than 16 generations (Amano et al., 2004). We investigated behavioral parameters using a first experimental group of aged-matched Ts1Cje males (n = 20) and their WT littermates (n = 20). Animals were group-housed (four per cage: two Ts1Cje and two WT littermates) and bred on a 12 h light/dark cycle (lights on at 7:00 a.m.) with *ad libitum* access to food and water. The exact ages for the various tests of our screening pipeline are shown in Table 1. Tests were carried out from least to most stressful, with larger recovery gaps given after forced swim and tail suspension tests. A few animals died in the gap between Porsolt forced swim test and tail suspension (1 WT and 2 Ts1Cje). These deaths were not restricted to a specific a phenotype and most likely due to aging as mice were above one year old for these tests. For this primary screening pipeline, experiments were performed between 9:00 a.m. and 6:00 p.m. (i.e. during the light phase of the maintenance cycle) and devices were cleaned with super hypochlorous water to prevent the influence of olfactory cues. All raw data and experimental information are available in the Mouse Phenotype Database (http://www.mouse-phenotype.org/). For every other behavioral (cohorts 2 and 3, see Table 1) or biochemical experiments, mice were group-housed (two to five per cage) with free access to food and water and maintained under a 12 h light/dark cycle (lights on at 8:00 a.m.). Cohorts 2 and 3 were composed of eleven Ts1Cje males and ten WT littermates for the home cage monitoring and three Ts1Cje males and four WT littermates for the tail suspension test. Each mouse was examined for a visual placing response to rule out blindness. All

experimental procedures and housing conditions were approved by the Animal Experiments Committees at RIKEN Institute, Fujita Health University and Kyoto Pharmaceutical University, and all animals were cared for and treated humanely in accordance with the Institutional Guidelines for experiments using animals.

2.2. General health and neurological screen

The righting, whiskers twitch, and ear twitch reflexes were evaluated. We acquired body weight and rectal temperature and checked a number of physical features, notably the presence or absence of whiskers or bald hair patches.

2.3. Open field test

Locomotor activity was measured in an open field task as previously described (Nakao et al., 2015). Mice were placed in the center of a 40 × 40 × 30 cm open field (Accuscan Instruments, Columbus, OH, USA). The test chamber was illuminated at 100 lux. The total distance traveled, vertical activity (rearing automatically detected by photobeam interruptions), time spent in the center area (20 × 20 cm) of the chamber, and beam-break counts for stereotypic behavior were recorded. Data were collected for 120 min.

2.4. Elevated plus maze test

The elevated plus maze test was conducted as previously described (Komada et al., 2008). The apparatus consisted of two open arms (25 × 5 cm) crossing two enclosed arms of the same size with 15 cm high transparent walls (O'Hara & Co., Tokyo, Japan). The arms and central square (5 × 5 cm) were made of white plastic plates, and the apparatus was placed 55

cm above the floor. To minimize the likelihood of animals accidentally falling from the apparatus, open arms were equipped with 3 mm high Plexiglas ledges. Mice were placed in the central square of the maze facing one of the closed arms and were left to explore the apparatus for 10 min. Data acquisition and analysis were performed automatically using ImageEP software (see 'Data analysis').

2.5. 24-hours locomotor activity monitoring in the home cage

Home cage activity over a 24-hours period was assessed using cage tops equipped with infrared sensors (Supermex - Muromachi Kikai, Tokyo, Japan). Mice were set in individual housing in their regular rearing cages placed in the Supermex rack for 3 days prior to the recording. Data were recorded for 24-hours, starting at 10 a.m. (light phase of the cycle). No movements were detected during periods of sleep, inactivity, or moderate self-grooming.

2.6. Social interaction in a novel environment

Social interaction in a novel environment was assessed as previously described (Nakao et al., 2015). Briefly, two mice of identical genotype that were previously housed in different cages were placed in a 40 × 40 × 30 cm open field and allowed to explore freely for 10 min. When the two mice made contact with each other and the distance traveled by either mouse was longer than 5 cm, the behavior was defined as an 'active contact'. Data acquisition and analysis were performed automatically using ImageSI software (see 'Data analysis').

2.7. Three-chamber sociability test

The three-chamber test for sociability is a widely used method to investigate the

complexity of social behaviors (Crawley, 2004; Moy et al., 2004; Nakao et al., 2015). The rectangular three-chamber apparatus was covered by a lid equipped with an infrared video camera (O'Hara & Co., Tokyo, Japan). The 20 × 40 × 22 cm chambers were separated by clear Plexiglas walls with small square openings (5 × 3 cm) to allow passage between chambers. A small circular wire cage was placed in each of the lateral chambers (11 cm height × 9 cm diameter with bars spaced 0.5 cm apart to allow nose-to-nose contacts). Eight non-familiar 8–10 weeks old C57BL/6J male mice were used as strangers for this test. The subject mouse was first placed in the central chamber and allowed to explore the chamber and empty cages for 10 min. One stranger mouse was then placed in one of the wire cages. The "stranger side" was randomized to prevent a side preference effect. The distance traveled, time spent in the chambers, and interaction time (amount of time spent within the 5 cm area surrounding the stranger's cage) was measured by video tracking. Data acquisition and analysis were performed automatically using ImageCSI software (see 'Data analysis').

2.8. Porsolt forced swim test

The Porsolt forced swim test was performed as previously described (Nakao et al., 2015). The apparatus consisted of four Plexiglas cylinders (20 cm height × 10 cm diameter; O'Hara & Co., Tokyo, Japan). The cylinders were filled with water at 23°C to a height of 7.5 cm. Mice were placed in the cylinders, and their behavior was recorded over a 10 min test period (days 1 and 2). Images were captured at one frame per second. For each pair of successive frames, the area (pixels) within which the mouse moved was measured. When the area was below the established threshold, the mouse was considered to be 'immobile'. When the area equaled or exceeded the threshold, the mouse was considered to be 'moving'. The optical

threshold was determined by adjusting the immobility measured by human observation. Immobility events lasting for less than 2 sec were not included in the analysis. Data acquisition and analysis were performed automatically using ImageTS software (see 'Data analysis'). Statistical significance was assessed using two-way ANOVA for repeated measures with "genotype" and "time" factors.

2.9. Light/Dark transition test

The Light/Dark transition test was conducted as previously described (Takao and Miyakawa 2006). A cage (21 × 42 × 25 cm) was divided into two sections of equal size by a partition with a door (O'Hara & CO., Tokyo, Japan). One chamber was brightly illuminated (390 lux), whereas the other chamber was dark (2 lux). Mice were placed into the dark chamber and allowed to explore freely for 10 min. Data acquisition and analysis were performed automatically using ImageLD software (see 'Data analysis' in main Materials and Methods section).

2.10. Motor function tests

Motor function tests, including grip strength, wire hang and rotarod tasks, were conducted as previously described (Nakao et al., 2015). A wire hang test apparatus (O'Hara & Co., Tokyo, Japan) was used to assess balance and grip strength. The apparatus consisted of a box (21.5 × 22 × 23 cm) with a wire mesh grid (10 × 10 cm) and a trigger-activated inversion that caused mice to grip the wire. Latency to fall was recorded with a 60 sec cut-off time. A grip strength meter (O'Hara & Co., Tokyo, Japan) was used to assess forelimb grip strength. Mice were lifted and held by their tail so that their forepaws could grasp the wire grid. The

mice were then gently pulled horizontally backward by the tail until they released the grid. The peak grip-force applied by the forelimbs of the mouse was recorded in Newtons (N). Each mouse was tested three times, and the highest value was used for statistical analysis. Motor coordination and balance were tested using an accelerating rotarod paradigm (UGO Basile Accelerating Rotarod, Varese, Italy). Mice were placed on an accelerating rod 3 cm in diameter (4 to 40 rpm over 5 min), and the latency to fall from the rod was recorded.

2.11. Hot plate test

The hot plate test was conducted as previously described (Nakao et al., 2015) to evaluate sensitivity to a painful stimulus. Mice were placed on a 55.0 ± 0.3°C hot plate (Columbus Instruments, Columbus, OH), and the latency to the first paw response was recorded with a 15-sec cut-off time. The hind-paw response was defined as either a foot shake or paw lick.

2.12. Startle response/prepulse inhibition

The startle response/prepulse inhibition test was conducted as previously described (Nakao et al., 2015). A startle reflex measurement system was used (O'Hara & Co., Tokyo, Japan). The test session began by placing a mouse in a Plexiglas cylinder where it was left undisturbed for 10 min. The duration of the white noise used as the startle stimulus was 40 msec for all trial types. The startle response was recorded for 400 msec (measuring the response every 1 msec) beginning with the onset of the prepulse stimulus. The background noise level in each chamber was 70 dB. The peak startle amplitude recorded during the sampling window was recorded. The test session consisted of six trials, i.e., two 'startle-stimulus-only' trials and four prepulse inhibition trials. The intensity of startle stimulus was

110 or 120 dB. In the prepulse inhibition trials, the startle stimulus was preceded by a prepulse sound (100 msec before the startle stimulus) at either 74 or 78 dB, resulting in four prepulse-startle combinations: 74–110 dB, 78–110 dB, 74–120 dB, and 78–120 dB. Six blocks of these six trials were presented in a pseudo-random order to each mouse. The average inter-trial interval was 15 sec (range: 10–20 sec).

2.13. Tail suspension test

The tail suspension test was conducted as previously described (Nakao et al., 2015). Mice were suspended 30 cm above the floor of a white plastic chamber (31 × 41 × 41 cm; O'Hara & Co., Tokyo, Japan) in a visually isolated area by adhesive tape placed ~1 cm from the tip of the tail. The animal's behavior was recorded for a 10 min test period, and images were captured at one frame per second. Similar to the Porsolt forced swim test, immobility was assessed with an established threshold using a computer program. Immobility events lasting for less than 2 sec were not included in the analysis. Data acquisition and analysis were performed automatically using ImageTS or ImageFZ2 software (see 'Data analysis' in main Materials and Methods section). Four WT and three Ts1Cje mice were recorded at 3 months old, nineteen WT and eighteen Ts1Cje mice were analyzed at 53–55 weeks old.

2.14. Data analysis

The programs used to analyze the behavioral data (ImageEP, ImageLD, ImageSI, ImageCSI ImageHA, ImageTS and ImageFZ2) were based on ImageJ (Image J Dev. Org, available at http://rsb.info.nih.gov/ij). The programs were modified for each test and are available through O'Hara & Co. Statistical significance was conducted using StatView (SAS

Institute, Cary, NC) or Excel statistics (ESUMI Co., Ltd, Japan). Data were analyzed using a paired *t*-test, the Student's *t*-test, one-way ANOVA, or two-way repeated-measures ANOVA unless otherwise specified. The values shown in graphs and reported in the text are expressed as the mean ± SEM.

2.15. Microdialysis

We used four Ts1Cje and four WT littermates males at 14–16 weeks-old. Mice were anesthetized using Somnopentyl (50 mg/kg) and stereotaxically implanted with a cannula (AG-4, Eicom, Kyoto, Japan) in the left hemisphere to guide the dialysis probe (2.0 mm active membrane length, 50,000 Da cut-off; A-I-4-02, Eicom). The striatum (anterior +0.50 mm, lateral ±2.0 mm, depth −3.5 mm from Bregma; Fig. 5A) was targeted according to common landmarks (Paxinos & Franklin, 2001). Mice were given one week of recovery. Probes were then inserted in freely moving mice and perfused with Ringer's solution (147.2 mM NaCl, 4.0 mM KCl, and 2.2 mM $CaCl_2$; pH 6.4) at a constant 2 µl/min flow rate for a total of 360 min. After an one-hour stabilization period, six consecutive fractions (20 min each) were collected to measure baseline levels. High K^+ Ringer's solution (50 mM NaCl, 100 mM KCl, and 2.2 mM $CaCl_2$; pH 6.2) was then perfused, and three high K^+ fractions (20 min each) were collected. The microdialysis fractions (40 µl) were collected every 20 min in 10 µl of 100 mM phosphate buffer (with 100 µM EDTA; pH 3.5) and immediately stored at −80°C. Monoamines and their metabolites were quantified by HPLC coupled with an electrochemical detection system (HITEC-500, Eicom, Kyoto Japan). For the simultaneous analysis of 11 compounds, samples were separated on a reversed-phase column (3.0 mm i.d. × 150 mm, EICOMPAK SC-5ODS, Eicom) using a mobile phase [0.1 M citrate-acetate buffer

(pH 3.5), 17% methanol, 190 mg/L sodium 1-octanesulfonate and 5 mg/L EDTA] pumped at a rate of 0.5 mL/min. The graphite electrode (WE-3G) working potential was set to +750 mV against an Ag/AgCl reference electrode. The column temperature was maintained at 25°C. For rapid analysis of DA, 5-HT and NA, an EICOMPAK CAX column (2.0 mm i.d. × 200 mm, Eicom) was used at 32°C with a graphite electrode potential set to +500 mV. The mobile phase [100 mM ammonium acetate buffer (pH 6.0), 50 mM sodium sulfate, 50 mg/L EDTA and 30% (vol/vol) methanol] flow rate was 0.25 mL/min. HPLC data were automatically collected and analyzed by PowerChrom software (eDAQ, Nagoya Japan). External standards were used to determine retention times, peak areas, and concentrations. Microdialysis probe positions were confirmed histologically.

2.16. Tissue Collection and Neurochemical Analysis

Eight WT and nine Ts1Cje mice at 11–14 weeks of age were euthanized by decapitation, and brains were immediately removed, frozen on dry ice, and stored at −80°C until sectioning. Coronal sections (150 μm) were cut at −20°C on a cryostat (Leica Microsystems, Nussloch, Germany). After Nissl staining, circular punches from the striatum and ventral forebrain were taken using either a complete 1.5 mm or half of a 2 mm diameter circular biopsy punch at an equivalent position in each sample, respectively (Kai Medical, Gifu Pref., Japan). A total of 16 punches were taken for the striatum [between AP coordinates +1.10 mm and +0.14 mm from Bregma, according to The Mouse Brain in Stereotaxic Coordinates (Paxinos & Franklin, 2001)], and 16 punches were collected from the ventral forebrain (AP: +1.34 mm to +0.74 mm) respectively (Fig. 5E and Supplementary Fig. S3). Tissue samples were stored at -80°C until assay.

Neurotransmitters were extracted from the punched biopsies by sonication in 70 μL of extraction buffer [0.1 M perchloric acid, 200 nM isoproterenol (ISO), 200 μM L-norleucine (NLE), and 5 μM ethylhomocholine]. ISO or NLE was used as the internal standards for monoamine and amino acid quantification, respectively. The total protein concentration was determined using a Bio-Rad Protein assay kit. The remainder of each sample was centrifuged for 15 min at 15,000 g, and the supernatant was filtered through a 0.22-μm Durapore PVDF filter (Millipore Corp., MA, USA). The filtrate was stored at −80°C for later HPLC analysis.

Monoamines in tissue extracts were measured by HPLC coupled to an electrochemical detection system (Eicom). For monoamines and metabolites analysis, samples were separated on a 3.0 × 150 mm EICOMPAK SC-5ODS column using a mobile phase [43.7 mM citrate, 39.3 mM sodium acetate, 17% methanol, 190 mg/L sodium 1-octanesulfonate, 5 mg/L EDTA, pH 3.5], pumped at 0.5 mL/min. The graphite working electrode (WE-3G) potential was set at +0.75 V and column temperature maintained at 25°C. For measurement of amino acids, samples were derivatized with o-phthalaldehyde for 30 s before gradient separation on a reverse-phase 3 × 150 mm HPLC column (Hypersil, 3 μm, C18, Keystone Scientific) using sodium acetate (35 mM, pH 5.9 adjusted with glacial acetic acid) and 1% (v/v) tetrahydrofuran as the aqueous solvent and 70% acetonitrile, 15% methanol, and 15% sodium acetate (35 mM final concentration), pH 7.65 (adjusted with glacial acetic acid) as the organic solvent. Flow rate was set at 0.6 ml/min. The column was maintained at 30°C. Analytes were detected by fluorometry. HPLC data were automatically collected and analyzed using EzChrom Elite (Scientific Software Inc., Tokyo, Japan) using regularly generated standard from external standards and normalization to internal standards.

2.17. Immunohistochemistry

We used three Ts1Cje and their three WT littermates males at 12–15 weeks-old. Mice were lethally anesthetized with a pentobarbital injection [0.3 mg/g body weight, intraperitoneal administration (i.p.)] and perfused transcardially with cold saline and cold 4% paraformaldehyde using a 24-gauge needle at a rate lower than 0.5 ml/min. Sections (6 μm) of 4% paraformaldehyde-fixed, paraffin-embedded brains were deparaffinized, rehydrated, and incubated in a 90°C preheated Retrievagen solution (BD Biosciences, Boston, MA, USA) for 10 min. For COMT, a mouse-on-mouse blocking kit (Vector Laboratories, Burlingame, CA, USA) was used to block mouse IgG. Slides were incubated with a blocking solution (10% goat serum and 0.3% Triton X-100 in PBS) containing avidin blocking solution (Vector Laboratories) for 1 h at room temperature. Next, sections were incubated with mouse anti-COMT (1:100, aa 26–141, BD Biosciences), rabbit anti-ALDH1A1 (1:200, ab23375, Abcam, Cambridge, UK), rabbit anti-tyrosine hydroxylase (1:50, NB300–109, Novus Biological, Littleton, CO, USA), or rabbit anti-AADC (1:100; AVIVA Systems Biology, San Diego, CA, USA) in a humidified chamber for 12 h at 4°C. Endogenous peroxidases were quenched by incubation in 0.3% hydrogen peroxide in PBS. Next, sections were incubated with biotinylated goat polyclonal secondary antibody (1:200; Vector Laboratories). Antibody–antigen complexes were revealed using a Vectastain Elite ABC kit (Vector Laboratories) and a metal-enhanced DAB substrate kit (Pierce/Thermo Scientific, Rockford, IL, USA). Nuclei were counterstained with hematoxylin.

2.18. Western blot

Striatal tissue isolated from five WT and five Ts1Cje mice at 12–15 weeks of age after

perfusion with ice-cold saline was homogenized in sonication buffer (10 mM phosphate buffer, pH 7.4, 0.5 mM dithiothreitol) supplemented with a complete protease inhibitor cocktail tablet (Roche Diagnostics, Indianapolis, IN, USA) and phosphatase inhibitors (Wako Pure Chemical Industries Ltd., Osaka, Japan). Proteins were extracted by a 30 sec sonication. After centrifugation at 15,000 rpm for 10 min at 4°C, the protein concentration in the supernatant was determined by the Bradford method. Five microgram aliquots of protein samples were denatured, subjected to SDS–4–20% polyacrylamide gel electrophoresis and then transferred electrically onto nitrocellulose membranes. After blocking the membranes with 3% skimmed milk (Wako Pure Chemical Industries Ltd.) in Tris-buffered saline containing 0.05% Tween-20 (TBS-T), the membranes were incubated with antibodies against COMT (mouse monoclonal, diluted at 1:10,000 with 3% skim milk/TBS-T; BD Biosciences), ALDH1A1 (rabbit polyclonal, 1:700 with 3.5% skim milk/TBS-T; Abcam), and β-actin (mouse monoclonal, 1:2,000 with 3% skim milk/TBS-T, Wako Pure Chemical Industries Ltd.) for 16 h at 4°C. After washing with TBS-T, the membrane was incubated with horseradish peroxidase-conjugated goat anti-rabbit IgG (Santa Cruz Biotechnology, Santa Cruz, CA, USA; 1: 5,000 with TBS-T) or goat anti-mouse IgG (Santa Cruz Biotechnology; 1:5,000 with TBS-T) for 1 h. After washing, immunoreactive bands were detected using Chemi-Lumi One Super (Nacalai Tesque, Inc., Kyoto, Japan) and a LAS-3000 mini image analysis system (Fujifilm, Tokyo, Japan). The band intensities were quantified with ImageJ.

3. Results

3.1. Ts1Cje mice show locomotor hyperactivity in unfamiliar environments

In order to evaluate the overall performance of Ts1Cje mice we used a comprehensive behavioral test battery after a quick assessment of the animal's general health. Pre-testing general inspection revealed a small yet significantly lower body weight of 24.65 ± 0.35 g in Ts1Cje compared to 26.58 ± 0.39 g in WT (one-way ANOVA, genotype effect, $F_{1, 38}$ = 13.694, p = 0.0007). Body temperature was not significantly different between Ts1Cje and their WT littermates (WT: 36.04 ± 0.13 °C; Ts1Cje: 35.83 ± 0.18 °C, one-way ANOVA, genotype effect, $F_{1, 38}$ = 0.895, p = 0.3502). No obvious abnormalities were found in either group in terms of gross morphology and basic neurological parameters (righting reflex, whisker twitch reflex, ear twitch reflex and response to key jangling).

To assess the locomotor activity of Ts1Cje mice in unfamiliar environments, we performed multiple behavioral tests. In the open field test, the distance traveled and vertical activity was markedly increased in Ts1Cje mice when compared with WT mice (Fig. 1A and B; two-way repeated-measures ANOVA, genotype effect, $F_{1, 38}$ = 13.450, p = 0.0007 and $F_{1, 38}$ = 17.713, p = 0.0002, respectively). Although not statistically significant, stereotypic counts tended to be higher in Ts1Cje mice (Fig. 1C; two-way repeated-measures ANOVA, genotype effect, $F_{1, 38}$ = 1.11, p = 0.2987). The time spent in the center of the open field was increased in Ts1Cje mice (Fig. 1D; two-way repeated-measures ANOVA, genotype effect, $F_{1, 38}$ = 15.323, p = 0.0004), suggesting that Ts1Cje mice are less anxious. In the elevated plus maze test, both the total distance traveled and the total number of arm entries were significantly increased in Ts1Cje mice (Fig. 1E and F; one-way ANOVA, genotype effect, $F_{1, 38}$ = 17.865, p = 0.0001 and $F_{1, 38}$ = 13.094, p = 0.0009, respectively). Significant increases in

the percentage of open arm entries and time spent in the open arms were observed in Ts1Cje mice (Fig. 1G and H; one-way ANOVA, genotype effect, $F_{1, 38} = 6.183$, p = 0.0174 and $F_{1, 38} = 8.042$, p = 0.0073, respectively). Taken together, these results indicate that Ts1Cje mice are hyperactive and possibly less anxious when compared with WT mice in novel environments.

3.2. Ts1Cje mice show decreased activity in familiar environments

As the activity of Ts1Cje mice was increased in tasks involving environmental novelty, we questioned whether in familiar environments a similar hyperactivity could be seen. Mice were monitored in their home cage activity for 24 hours, covering a full light/dark cycle. Overall, Ts1Cje mice were significantly less active than their WT littermates in the context of their home cage (Fig.1I, two-way repeated-measures ANOVA, genotype effect: $F_{1, 19} = 19.79$, $p < 0.0001$). This significant hypo-activity was seen specifically during the dark phase where mice from both genotypes were most active (two-way repeated-measures ANOVA, genotype effect, $F_{1, 19} = 25.28$, $p < 0.0001$). During the light phase mice were relatively immobile and no significant difference were seen between WT and Ts1Cje mice (two-way repeated-measures ANOVA, genotype effect, $F_{1, 19} = 0.4379$, p = 0.5087). Unlike what was seen in novel environments, Ts1Cje mice are thus hypoactive in familiar environments.

3.3. Ts1Cje mice show increased sociability in unfamiliar environments and with novel partners

To assess the sociability of Ts1Cje mice in different environmental conditions we used two different testing paradigms.

We first looked at sociability in an unfamiliar environment. For that purpose we

measured the social interactions in a novel open field without habituation prior to the test (paired with a separately housed mouse of the same genotype). Ts1Cje mice traveled significantly longer distances than their WT littermates confirming a novelty-induced hyperactivity (Fig. 2A; one-way ANOVA, genotype effect, $F_{1, 18} = 16.443$, $p = 0.0007$). Both the total duration and number of contacts were significantly increased in Ts1Cje-Ts1Cje pairs compared to WT-WT pairs (Fig. 2B and C; one-way ANOVA, genotype effect, $F_{1, 18} = 15.191$, $p = 0.0011$ and $F_{1, 18} = 27.415$, $p < 0.0001$, respectively). The mean duration per contact was however similar between genotypes (Fig. 2D; one-way ANOVA, genotype effect, $F_{1, 18} = 0.524$, $p = 0.4783$). The total duration of active contacts (see Materials and Methods) in Ts1Cje mice was longer than that of WT mice (Fig. 2E; one-way ANOVA, genotype effect, $F_{1, 18} = 26.334$, $p < 0.0001$).

We used the 3-chamber task to investigate the sociability of Ts1Cje mice towards a novel partner after habituation to the environment (Fig. 2F). Mice were allowed to freely explore for 10 minutes to habituate to the apparatus and were then immediately tested for sociability. No side preference was observed in either group during the habituation phase (data not shown). During the social preference phase (Fig. 2F) the total distance traveled was not significantly different between genotypes, suggesting a successful habituation to the apparatus (Fig. 2G; one-way ANOVA, genotype effect, $F_{1, 38} = 1.562$, $p = 0.219$). The average moving speed was faster in Ts1Cje mice (Fig. 2H; one-way ANOVA, genotype effect, $F_{1, 38} = 11.458$, $p = 0.0017$). Both WT and Ts1Cje mice spent significantly more time in the stranger compartment than in the empty compartment (Fig. 2I; paired *t*-test, genotype effect, WT mice; $t_{19} = -4.245$, $p = 0.0004$, and Ts1Cje mice; $t_{19} = -7.707$, $p < 0.0001$) without significant genotype effect (Fig. 2I; two-way repeated-measures ANOVA, genotype effect, $F_{1, 38} = 1.900$,

p = 0.1761; genotype × chamber interaction, $F_{2, 76}$ = 2.354, p = 0.1019). Whereas no significant difference was seen in the time spent investigating the empty cage, Ts1Cje mice spent significantly more time investigating the stranger's cage than their WT littermates (Fig. 2J; one-way ANOVA, genotype effect, empty side: $F_{1, 38}$ = 0.862, p = 0.3591, and stranger side: $F_{1, 38}$ = 12.595, p = 0.001; two-way repeated-measures ANOVA, genotype effect, $F_{1, 38}$ = 9.530, p = 0.0038; genotype × cage interaction, $F_{1, 38}$ = 8.983, p = 0.0048). These results indicate that even in familiar environments Ts1Cje mice show increased sociability if the partners are novel.

3.4. Decreased depression-like behavior in Ts1Cje mice

We assessed the depression-like behavior of Ts1Cje mice using the Porsolt forced swim test. Ts1Cje mice were significantly less immobile than WT mice on both day 1 and 2 (Fig. 3A; two-way repeated-measures ANOVA, genotype effect, $F_{1, 38}$ = 6.058, p = 0.0185, and $F_{1, 38}$ = 16.786, p = 0.0002, respectively; two-way repeated measures ANOVA, genotype × time interaction, $F_{9, 342}$ = 1.330, p = 0.2201, and $F_{9, 342}$ = 3.079, p = 0.0014, respectively). WT mice started Day 2 with a high immobility percentage (first two minutes on Day 2), and interestingly, Ts1Cje mice were considerably more mobile during this time (one-way ANOVA followed by Fisher's PLSD, genotype effect, 1 min: $F_{1, 38}$ = 14.162, p = 0.0006, and 2 min: $F_{1, 38}$ = 15.53, p = 0.0003, respectively). This effect may be partly due to the impaired short- to mid-term memory or hyperactivity of Ts1Cje mice. Accordingly, the total traveled distance during Days 1 and 2 was significantly increased in Ts1Cje mice (Fig. 3B; two-way repeated-measures ANOVA, genotype effect, $F_{1, 38}$ = 27.086, p < 0.0001, and $F_{1, 38}$ = 31.576, p < 0.0001, respectively; two-way repeated measures ANOVA, genotype × time interaction,

$F_{9, 342}$ = 1.690, p = 0.0901, and $F_{9, 342}$ = 3.535, p = 0.0003, respectively). This observation was corroborated by a mild decrease in immobility in the tail suspension test at one year old within the main screening process, but was not significantly supported by a preliminary batch of 11–16 weeks old naïve mice that have not been used in a series of behavior tasks (Supplementary Fig.S1; two-way repeated-measures ANOVA, genotype effect, $F_{1, 5}$ = 0.035, p = 0.8527; genotype × time interaction, $F_{9, 50}$ = 0.6958, p = 0.7093). These results suggest a mildly decreased tendency to give up in Ts1Cje mice; however, the hyperactivity, age and past experience of the mice may have contributed to the result.

3.5. Other behavioral abnormalities in Ts1Cje mice

In the light/dark transition test, Ts1Cje mice spent more time in the dark box (Supplementary Fig. S2A; one-way ANOVA, genotype effect, $F_{1, 38}$ = 38.977, p < 0.0001) and showed a lower number of light/dark transitions than their WT littermates (Supplementary Fig. S2B; one-way ANOVA, genotype effect, $F_{1, 38}$ = 11.151, p < 0.0019). The total distance traveled of Ts1Cje mice was lower in the light box and higher in the dark box (Supplementary Fig. S2C; one-way ANOVA, genotype effect, $F_{1, 38}$ = 19.982, p < 0.0001, $F_{1, 38}$ = 5.481, p = 0.0246, respectively). These results suggest higher anxiety in Ts1Cje mice in this behavioral test, which is in contrast to their reduced anxiety-like behavior in the open field and elevated plus maze.

Motor function and nociception were assessed by grip strength, wire hang, rotarod and hot plate tests. Although no significant difference was observed between WT and Ts1Cje mice in grip strength (Supplementary Fig. S2D; one-way ANOVA, genotype effect, $F_{1, 38}$ = 0.208, p = 0.6508), the latency of Ts1Cje mice to fall in the wire hang test was significantly

shorter (Supplementary Fig. S2E; one-way ANOVA, genotype effect, $F_{1, 38}$ = 12.130, p = 0.0013). Ts1Cje mice also showed shorter latency to fall in the rotarod motor coordination task (Supplementary Fig. S2F; two-way repeated-measures ANOVA, genotype effect, $F_{1, 38}$ = 13.222, p = 0.0008). In the hot plate test, there was a tendency for Ts1Cje mice to have a longer latency to respond, but this did not reach statistical significance (Supplementary Fig. S2G; one-way ANOVA, genotype effect, $F_{1, 38}$ = 3.973, p = 0.0535). Taken together, these results show impaired motor function and a tendency for a deficit in nociception. We also submitted Ts1Cje mice to the startle response/PPI test to evaluate sensorimotor gating. Ts1Cje mice showed a drastically smaller amplitude in their acoustic startle response than WT mice (Supplementary Fig. S2H; two-way repeated measures ANOVA, genotype effect, $F_{1, 38}$ = 25.996, p < 0.0001). However, PPI itself was not significantly affected (Supplementary Fig. S2I; two-way repeated measures ANOVA, genotype effect, 110dB startle, $F_{1, 38}$ = 1.049, p = 0.3122; 120dB startle, $F_{1, 38}$ = 0.031, p = 0.8609). Overall these data suggest a deficit in motor function that could be relevant to the muscular hypotonia commonly observed in persons with DS (Epstein, 2001).

3.6. Increased basal extracellular and total content of dopamine and serotonin in Ts1Cje mice

As locomotor hyperactivity is often associated with enhanced striatal dopaminergic neurotransmission (Giros et al., 1996), we at first measured extracellular monoamines in the striatum from WT and Ts1Cje mice at 14–16 weeks of age by microdialysis (Fig. 4A–D). Under basal conditions in freely moving mice, the extracellular concentration of dopamine (DA) was significantly increased in the adult Ts1Cje striatum (Fig. 4B, Table S2; *t*-test,

genotype effect, t_6 = 2.866, p = 0.0286). Furthermore, the extracellular concentration of serotonin (5-HT) in the Ts1Cje striatum showed a strong trend toward an increase (Fig. 4C, Table S2; *t*-test, genotype effect, t_6 = 2.417, p = 0.0521). No significant difference was observed in basal noradrenaline (NA) overflow (Fig. 4D, Table S2; *t*-test, genotype effect, t_6 = 0.6285, p = 0.5528). High-K^+ stimulation (100 mM K^+) during microdialysis, which induces massive neurotransmitter release locally, was used to quantify the maximum output capacity. The levels of DA, 5-HT, and NA were comparable in Ts1Cje and WT mice (Supplementary Fig. S3; *t*-test, genotype effect, t_6 = 0.4473, p = 0.6704; t_6 = 0.2069, p = 0.8429; and t_6 = 1.3701, p = 0.2197, respectively).

We quantified monoamine levels in tissue extracts from the striatum and ventral forebrain (Fig. 4E–H, Supplementary Fig. S4, and Supplementary Table S2). The protein content in the excised tissue samples from Ts1Cje mice was slightly lower than that from WT, but the difference was not statistically significant (WT/striatum: 9.41 ± 0.57 mg/mL vs. Ts1Cje/striatum: 8.19 ± 0.48 mg/mL, t_{15} = 1.662, p = 0.1173; WT/ventral forebrain: 6.59 ± 0.7 mg/mL vs. Ts1Cje/ventral forebrain: 5.33 ± 0.33 mg/mL, t_{15} = 1.69, p = 0.1116). Although the reason behind the decreased tendency in protein content in excised tissue from Ts1Cje mice is unknown, we did not detect a distinct decreased number of Nissl cells in stained brain sections (data not shown). The total amount of DA showed a tendency toward an increase for both of the measured brain regions in Ts1Cje mice but without reaching statistical significance (Fig. 4F, Supplementary Table S2; *t*-test, genotype effect, striatum: t_{15} = 1.671, p = 0.1155 and ventral forebrain: t_{15} = 1.185, p = 0.2545, respectively). Levels of 5-HT were significantly higher in the striatum and ventral forebrain of Ts1Cje mice (Fig. 4G, Supplementary Table S2; *t*-test, genotype effect, striatum: t_{15} = 2.8, p = 0.0135 and ventral

forebrain: t_{15} = 3.247, p = 0.0054, respectively). NA level was slightly, yet not significantly increased in the Ts1Cje striatum and significantly increased in the ventral forebrain (Fig. 4H and Supplementary Table S2; *t*-test, genotype effect, striatum: t_{15} = 1.335, p = 0.2019 and ventral forebrain: t_{15} = 2.294, p = 0.0366, respectively).

3.7. Increased levels of phenylalanine and tyrosine, monoamine turnover and abnormal expression of their catabolic enzymes in Ts1Cje mice

DA is biosynthesized from the degradation of phenylalanine (Phe) and tyrosine (Tyr) by tyrosine hydroxylase (TH) and aromatic L-amino acid decarboxylase (AADC), and degraded to homovanillic acid (HVA) by three enzymes, monoamine oxidase (MAO), aldehyde dehydrogenase (ALDH), and catechol-*O*-methyltransferase (COMT) (Fig. 5A). Amino acid concentrations were measured from tissue extracts of the Ts1Cje striatum and ventral forebrain. Both Tyr and Phe were increased in the striatum (Fig. 5B and C; *t*-test, genotype effect, Tyr: t_{15} = 4.062, p = 0.0010 and Phe: t_{15} = 4.197, p = 0.0008, respectively). In the ventral forebrain, both Tyr and Phe were significantly increased (*t*-test, genotype effect, Tyr: t_{15} = 2.589, p = 0.0206 and Phe: t_{15} = 2.622, p = 0.0192, respectively) (Supplementary Table S3). The concentrations of aspartate (Asp), serine (Ser), glutamate (Glu) and alanine (Ala) showed a tendency toward an increase in Ts1Cje mice; however, the difference did not reach statistical significance. The concentration of glycine (Gly) was significantly increased in the ventral forebrain of Ts1Cje mice (Supplementary Table S3).

We quantified monoamine metabolites in microdialysates and in tissue extracts from the striatum and ventral forebrain (Fig. 5D and E, Supplementary Table S4). Interestingly, the concentration of 3-MT, an indicator of DA release (Wood et al., 1982), was significantly

increased in the Ts1Cje striatum, supporting an enhanced DA overflow observed in the microdialysis experiment (Fig. 5D). The total amount, but not extracellular amount, of HVA was also increased in Ts1Cje striatum (Fig. 5E), whereas the amount of DOPAC was relatively unaffected in the Ts1Cje striatum (Supplementary Table S4). The level of 5-hydroxyindoleacetic acid (5-HIAA), a 5-HT catabolite, was significantly higher in the striatum and ventral forebrain extracts from Ts1Cje mice (Supplementary Table S4).

The HVA/DA ratio in striatal tissue extracts, used as an index of DA catabolism, was significantly increased in Ts1Cje mice (Supplementary Fig. S5A; *t*-test, genotype effect, HVA/DA: $t_{15} = 3.194$, p = 0.006). The HVA/DOPAC ratio was also significantly increased, whereas the DOPAC/DA ratio in tissue extracts showed a mild but non-significant decrease in the Ts1Cje striatum (Supplementary Fig. S5A; *t*-test, genotype effect, HVA/DOPAC: $t_{15} = 3.361$, p = 0.0043 and DOPAC/DA: $t_{15} = 1.713$, p = 0.1073, respectively). In contrast, 3-MT/DA and HVA/3-MT ratios were not different between genotypes (Supplementary Fig. S5A; *t*-test, genotype effect, 3-MT/DA: $t_{15} = 0.447$, p = 0.6615 and HVA/3-MT: $t_{15} = 1.408$, p = 0.1795, respectively). Overall, these results indicate that both DA production and degradation are enhanced, especially via the DOPAC pathway, thus resulting in a higher turnover in the Ts1Cje brain. Additionally, the 5-HIAA/5-HT ratio, which is an index of 5-HT turnover, was significantly increased in the Ts1Cje striatum but not ventral forebrain (Supplementary Fig. S5B; *t*-test, genotype effect, ventral forebrain: $t_{15} = 1.21$, p = 0.2452 and striatum: $t_{15} = 3.272$, p = 0.0051, respectively). Thus, there is a disturbance in DA and 5-HT in the Ts1Cje brain, particularly in the striatum.

We immunohistochemically examined TH, AADC, COMT, and ALDH (Fig. 5A, Fig. 6A and B, and Supplementary Figs. S6 and S7). There was no detectable difference in TH

between genotypes (Supplementary Fig. S6A–D). AADC was mildly lower in Ts1Cje mice (Supplementary Fig. S6E–H). COMT was markedly enhanced in the striatum and prefrontal cortex (Fig. 6A and Supplementary Fig. S7A and B). In contrast, ALDH was mildly lower in Ts1Cje mice (Fig. 6B and Supplementary Fig. S7C and D). We performed western blotting using striatum brain lysates from both genotypes (Fig. 6C and D). Densitometric quantification of band intensities revealed that the amount of COMT protein was significantly increased in the Ts1Cje striatum (Fig. 6D, left; *t*-test, genotype effect, $t_8 = 2.782$, $p = 0.0239$), whereas the level of ALDH protein was significantly decreased in the Ts1Cje striatum (Fig. 6D, right; *t*-test, genotype effect, $t_8 = 2.61$, $p = 0.0312$). These data are consistent with the immunohistochemistry of COMT and ALDH as well as the lower DOPAC/DA ratio in the Ts1Cje striatum (Supplementary Fig. S5A).

4. Discussion

Using a comprehensive battery of behavioral tests, we identified environmental novelty stimuli-triggered hyperactivity, increased sociability, and decreased depression-like behavior in Ts1Cje mice. Our neurochemical and immunohistochemical results further suggested that Ts1Cje mice show an abnormal increase in DA and 5-HT combined with an enhanced metabolism of these transmitters, which may help explain the affective and emotional abnormalities observed in these mice.

The locomotor hyperactivity of Ts1Cje mice was consistently observed in different behavior tasks: open field, elevated plus maze, light/dark transition, social interaction in a novel setup, and Porsolt forced swim test. In contrast, Ts1Cje mice turned out to be

hypoactive in familiar environments. These observations suggest that hyperactivity in Ts1Cje mice is triggered by mild stress such as a novel environment or environmental changes. Such response to environmental novelty is however not seen when spontaneous activity is assessed in the darkness (Sago et al., 1998) suggesting that luminosity is an important component of this novelty-induced hyperactivity in Ts1Cje mice. Locomotor hyperactivity was also reported in Ts65Dn mice (Reeves et al., 1995; Coussons-Read et al., 1996). Ts1Rhr mice however did not show significant changes in total distanced traveled when placed in a novel open field (Belichenko et al., 2009). Ts65Dn and Ts1Cje but not Ts1Rhr harbor overlapping MMU16 triplications and commonly show novelty-induced hyperactivity; thus, some of the genes responsible for the hyperactivity phenotype are likely located within the Ts1Cje specific trisomic region (Supplementary Fig. S8). In order to further investigate genotype-phenotype relationship and to test the involvement of candidate genes within the Ts1Cje specific trisomic region, a subtractive approach by crossing heterozygous knockout mice for a given candidate gene and Ts1Cje mouse can be used to genetically normalize the targeted gene's copy number (Supplementary Fig. S9, strategy used in Raveau et al., 2017).

We also identified novelty-induced disturbances of social behavior in the Ts1Cje model. When presented to unfamiliar partners in either new environment (open field) or after a short habituation period to the 3-chamber arena, young adult Ts1Cje mice showed enhanced sociability. Though very few reports focusing on social performance in human DS are available so far, children with DS are often perceived as sociable and outgoing (Gibbs and Thorpe, 1983). The enhanced sociability observed in Ts1Cje is thus mimicking what is seen in these children.

Ts1Cje mice also showed conflicting results in anxiety-like behavior related tasks. On

one hand, the time they spent in the center of the open field or in the open arms in the elevated plus maze are usually interpreted as a sign of decreased anxiety. In the light/dark transition task however, Ts1Cje mice showed signs of increased anxiety materialized by a longer time spent in the dark part of the box. One explanation for these observations is that the strong light intensity used in the light/dark box task could be more aversive than the elevation in the plus maze test or the milder luminosity used in the open field task. Such discrepancies between performances in light/dark transition and elevated plus maze tasks can in some cases reflect panic-like escape (Hattori et al., 2012, Holmes et al., 2000). We however doubt that this is the case in Ts1Cje mice as we did not observe attempts to escape in the different tests we performed, but also because a reduction in anxiety-like behavior has been reported in a different DS model, Ts65Dn (Coussons-Read and Crnic, 1996). Interestingly, this reduced anxiety can be attenuated by an antioxidant α-tocopherol-supplemented diet, which reverses aberrant lipid peroxidation in Ts65Dn mice (Shichiri et al., 2011). We previously identified a dramatic increase in lipid peroxidation due to enhanced oxidative stress in Ts1Cje adult brain (Ishihara et al., 2009). The co-occurrence of decreased anxiety-like behavior and increased oxidative stress in these two models and the successful recovery in Ts65Dn mice by anti-oxidant supplementation suggest a correlation between decreased anxiety and increased oxidative stress in DS.

One concern when working with Ts1Cje model is the presence of a seven genes monosomy on the distal end of mouse chromosome 12 (Duchon et al., 2011). Among these, only three show a significant change in expression level in cortical and hippocampal extracts (*Itgb8*, *Tmem196* and *Dnahc11*; Guedj et al., 2015), none of which has been shown to have an impact on the behavioral and biochemical parameters that we investigated in the present study.

Moreover, the fact that the phenotypes we identified in the Ts1Cje model have been seen in persons with DS makes it very unlikely that this monosomic fragment could be causing these defects.

Data from our tissue-punch experiment revealed that the monoamine and amino acid content showed a tendency to be higher in Ts1Cje mice. Notably, all of the amino acids examined were increased in the Ts1Cje brain. Specifically, Tyr and Phe in both brain regions examined and Gly in the ventral forebrain were significantly increased in Ts1Cje mice. Although the reason behind the decreased tendency in protein content in excised tissue from Ts1Cje mice is unknown, we did not detect a distinct decreased number of Nissl cells in stained brain sections.

Reports on DA metabolism in brain samples from DS patients have been rather controversial. Slight but non-significant increases in DA and HVA in the temporal and frontal cortex were described (Godridge et al., 1987), whereas another report showed decreased levels of DOPAC and a mild but non-significant decrease in DA in the temporal cortex (Risser et al., 1997). Although several reports describe abnormally high COMT activity in erythrocytes from persons with DS (Gustavson et al., 1973, 1982), this remains controversial (Brahe et al., 1985) and no data regarding COMT levels in the brains of patients with DS is available. DA was decreased in the brains of elder DS patients but not 27 year-olds with DS (Yates et al., 1983). The discrepancies in human studies may be due to age-specific changes and that samples were extracted post-mortem (after natural death). Neurochemical parameters are largely understudied in mouse models of DS; however, one study showed that the number of dopaminergic cells in the tegmental area and noradrenergic neurons in the locus coeruleus (LC) is unaffected in Ts65Dn mice (Megías et al., 1997). Our present microdialysis and

tissue-punch experiments revealed that extracellular DA in freely behaving Ts1Cje mice is increased and its metabolism is enhanced in the striatum. Indeed, both precursors (Phe and Tyr) and metabolites (3-MT and HVA) were increased in Ts1Cje tissue extracts, which supports the increased extracellular DA levels observed here in Ts1Cje mice. COMT expression was increased in Ts1Cje mice, whereas ALDH expression was lower in Ts1Cje mice. Similarly, a decrease in ALDH expression was reported in DS patients (Lubec et al., 1999). In our present study, the decreased and increased ratios of DOPAC/DA and HVA/DOPAC in Ts1Cje striatum are consistent with the decreased and increased immunoreactivities for ALDH and COMT, respectively. In contrast, the ratios of 3-MT/DA and HVA/3-MT were not significantly different between genotypes. These observations suggest that the abnormal expression of the catabolic enzymes for DA is not merely caused by a compensatory regulation. Although the mechanism remains unclear, overall DA metabolism was enhanced and the overflow of DA was increased in Ts1Cje mice.

Perturbations in the serotonergic system are suggested to play a role in anxiety and depression. Indeed, genetic variants for the 5-HT transporter gene leading to decreased serotonergic signaling are known risk factors in patients with anxiety (Gordon and Hen, 2004) and selective 5-HT re-uptake inhibitors (SSRI) are commonly used as anti-depressive treatments. So far, very few reports tackled depression, anxiety and/or serotonin signaling in DS in human and model mice, and their conclusions remain rather controversial. Whereas early reports described decreases in serotonin levels in post-mortem brain tissue from DS patients, these samples also showed signs of Alzheimer's disease, especially amyloid plaques and neurofibrillary tangles (Godridge et al., 1987; Risser et al., 1997). A decrease in serotonin level was also seen in the brain from aged Ts65Dn mice (Salehi et al. 2009). In frontal cortex

from young Ts65Dn mice, serotonin concentration was however found significantly increased and blocking 5HT2a receptors in these mice successfully rescued behavioral phenotypes (Heller et al. 2014). The susceptibility to anxiety and depression within the population with DS remains unclear. As extensively reviewed by Walker and colleagues (Walker et al. 2011), whereas a few studies suggested increases in depression cases in persons with DS, a more recent and more comprehensive population-based study describes a decreased incidence and suggests DS to actually be protective for depression (Mantry et al. 2008).

Our work supports this latter conclusion and the findings reported from the analysis of young Ts65Dn brain samples. Our microdialysis and tissue-punch analyses revealed increased 5-HT levels in the Ts1Cje striatum and ventral forebrain, as well as decreased depression-like behavior in the Porsolt forced swim task in young Ts1Cje mice. The tail suspension test, also commonly used as an indicator for depression-like behavior, did not show significant differences between young Ts1Cje and their WT littermates. Interestingly, serotonin deficient mice show a phenotype opposite to the Ts1Cje model: an increase in depression-like behavior in the Porsolt forced swim but no alterations in the tail suspension test (Mosienko et al. 2012). Taken together, these results suggest that the increased 5-HT levels in the brains from Ts1Cje mice may be directly responsible for their decreased depression-like behavior. In addition, although Ts1Cje performance in the tail suspension was normal at 3 months old, they showed a significant decrease in depression-like behavior in this task at 1 year old. This result illustrates that age-related factors are likely affecting the behavioral outcome in DS mice behavior.

The increased 5-HT concentrations in Ts1Cje brains could also participate in the other aspects of DS behavioral abnormalities. For instance, individuals taking the SSRI drug

citalopram showed increased cooperative behavior during a trial game when compared with a placebo group (Tse and Bond, 2002). The authors concluded that SSRI administration modulates social aspects of behaviors and increases affiliative behaviors. The increased social contacts in Ts1Cje mice may be caused by the increase in 5-HT.

Noradrenergic neurotransmission plays an important role in learning and memory, and neuronal loss in the LC, the major source of noradrenergic projections to the entire brain, was observed in aged individuals with DS and 6 month-old Ts65Dn mice (Mann et al., 1985; Salehi et al., 2009). In contrast, the concentration of NA is significantly elevated in the cerebrospinal fluid (CSF) of young adults with DS (Schapiro et al., 1987). Supporting this latter observation, we determined that the NA content was increased in the ventral forebrain of 3 month-old Ts1Cje mice. Although the NA concentration from young adults with DS is still unclear, our results suggest that it is likely not decreased. More extensive investigation should thus be considered before implementing NA agonist-based treatments in DS (Salehi et al., 2009). Monoamine metabolism alterations still require further investigation in order to understand how they are involved in the developmental and functional deficits in the brains of DS patients.

In summary, we identified environmental stimuli-triggered hyperactivity, increased sociability and decreased depression like-behavior in Ts1Cje mice. These features of Ts1Cje mice may be due to the increased overflow of dopamine and serotonin. These findings contribute to the understanding of affective and emotional features of DS patients and may be useful for the development of safer therapeutic approaches (Shimohata et al., 2017).

5. Figure

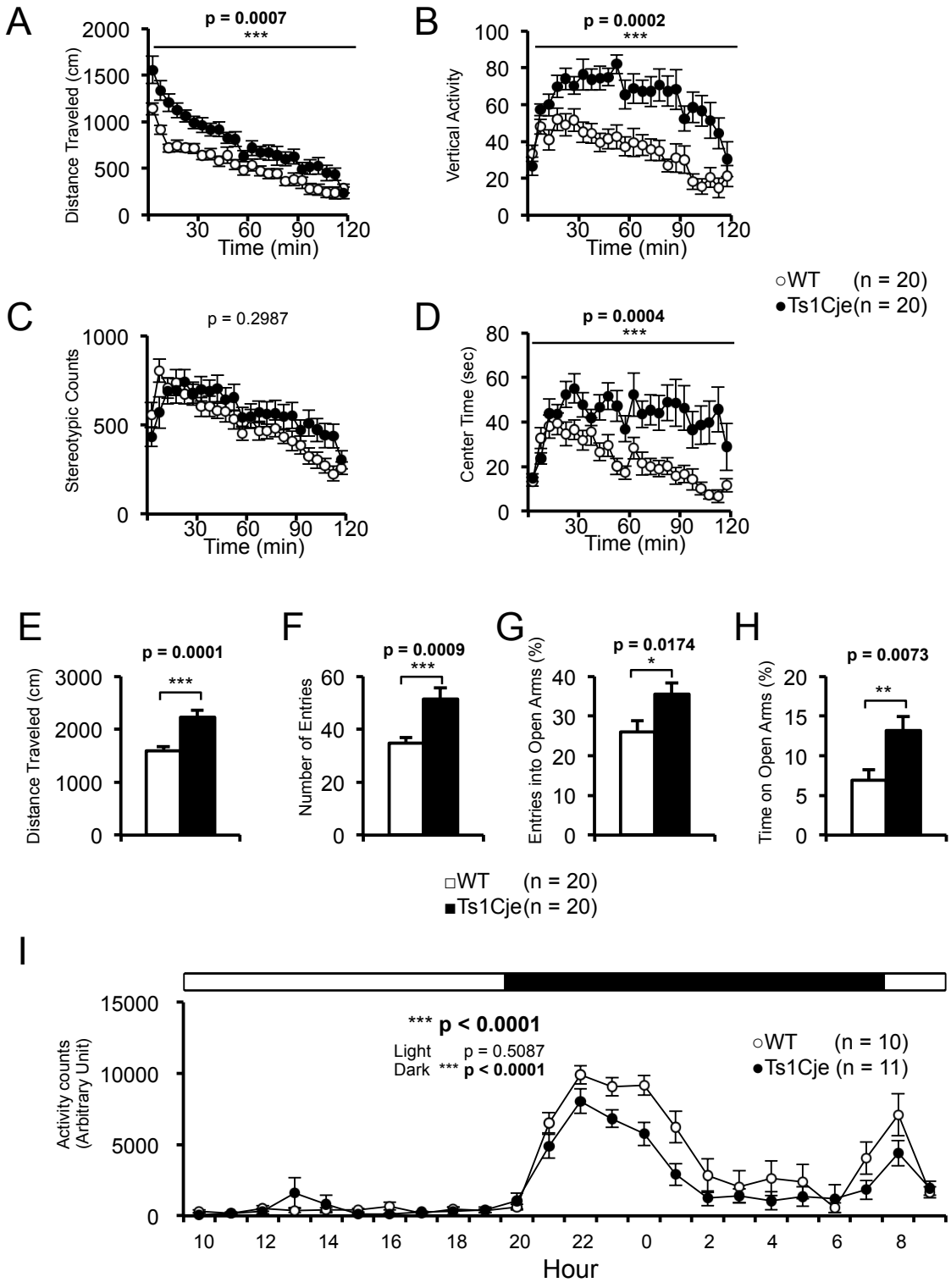
A
p = 0.0007
***
Distance Traveled (cm)
Time (min)
B
p = 0.0002
***
Vertical Activity
Time (min)
○WT (n = 20)
●Ts1Cje(n = 20)
C
p = 0.2987
Stereotypic Counts
Time (min)
D
p = 0.0004
***
Center Time (sec)
Time (min)
E
p = 0.0001
***
Distance Traveled (cm)
F
p = 0.0009
***
Number of Entries
G
p = 0.0174
*
Entries into Open Arms (%)
H
p = 0.0073
**
Time on Open Arms (%)
□WT (n = 20)
■Ts1Cje(n = 20)
I
*** p < 0.0001
Light p = 0.5087
Dark *** p < 0.0001
○WT (n = 10)
●Ts1Cje (n = 11)
Activity counts (Arbitrary Unit)
Hour

Figure 1. Increased environmental stimuli-induced locomotor hyperactivity in Ts1Cje mice.

(A–D) Open field test. Total distance traveled (A), vertical activity (i.e., rearing) (B) and time spent in the center (D) were significantly increased in Ts1Cje mice at 10–13 weeks of age, whereas stereotypic counts (C) were comparable to WT mice. (E–H) Elevated plus maze test. Total distance traveled (E), total number of arm entries (F), percentage of entries into open arms (G) and percentage of spent time in the open arms (H) were significantly higher in Ts1Cje mice at 11–13 weeks of age, indicating increased locomotor activity and suggesting decreased anxiety-like behavior. (I) Home cage activity test. Spontaneous home cage activity was monitored for 24 hours. The upper bar indicates the day-night cycle (dark bar for night and open bar for day time). Locomotor activity in Ts1Cje mice at 12–13 weeks of age was significantly decreased during the dark phase of the cycle compared to their WT littermates. P-values indicate a genotype effect in a one-way ANOVA (E–H) or two-way repeated-measures ANOVA (A–D and I). Sample numbers correspond to number of mice. Data are shown as the mean (± SEM); * $p < 0.05$, ** $p < 0.01$, and *** $p < 0.001$.

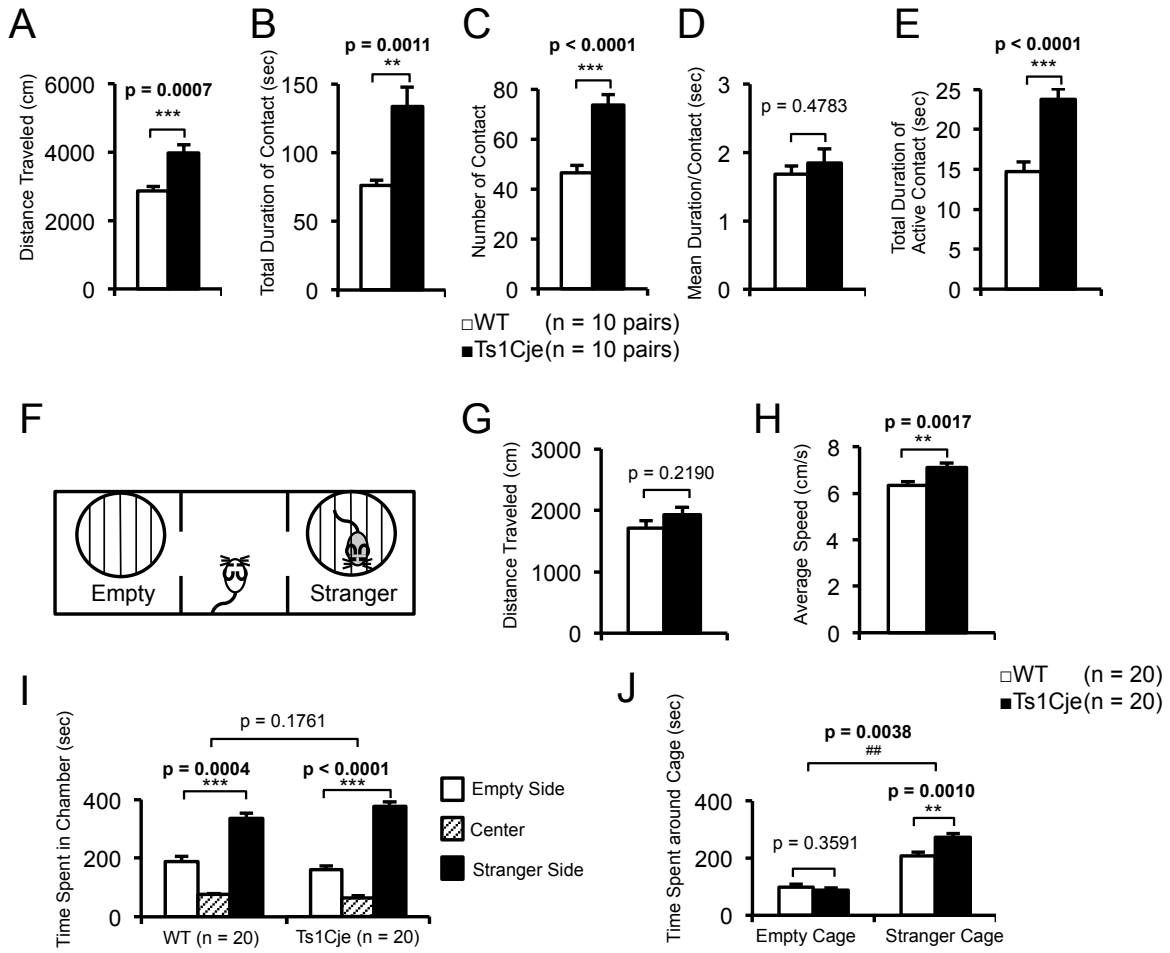

Figure 2. Increased sociability of Ts1Cje mice in unfamiliar environments. (A–E) Social interaction test in a novel environment (open field). Total distance traveled (A), total duration of contacts (B), number of contacts (C) and total duration of active contacts (E) were significantly increased in Ts1Cje mice at 12–14 weeks of age, whereas the mean duration per contact (D) was comparable to WT littermates. (F–J) Three-chamber sociability test. (F) Diagram of the three-chamber apparatus used in the sociability task. (G–J) During this test, the distance traveled (G) was similar between genotypes at 13–16 weeks of age; however, Ts1Cje mice showed an increased average move speed (H). (I) Both WT and Ts1Cje mice spent significantly more time in the stranger's compartment than the empty or central

compartments. Ts1Cje mice spent more time investigating the stranger's cage than WT littermates (J). P-values indicate a genotype effect in a paired *t*-test (I) or one-way ANOVA (A–E, G, H and J) or two-way repeated-measures ANOVA (I and J). Sample numbers correspond to number of pairs of equivalent genotype (A-E) or number of mice (F-J). Data are shown as the mean (± SEM); * $p < 0.05$, ** $p < 0.01$, and *** $p < 0.001$, and $^{\#\#}$ $p < 0.01$.

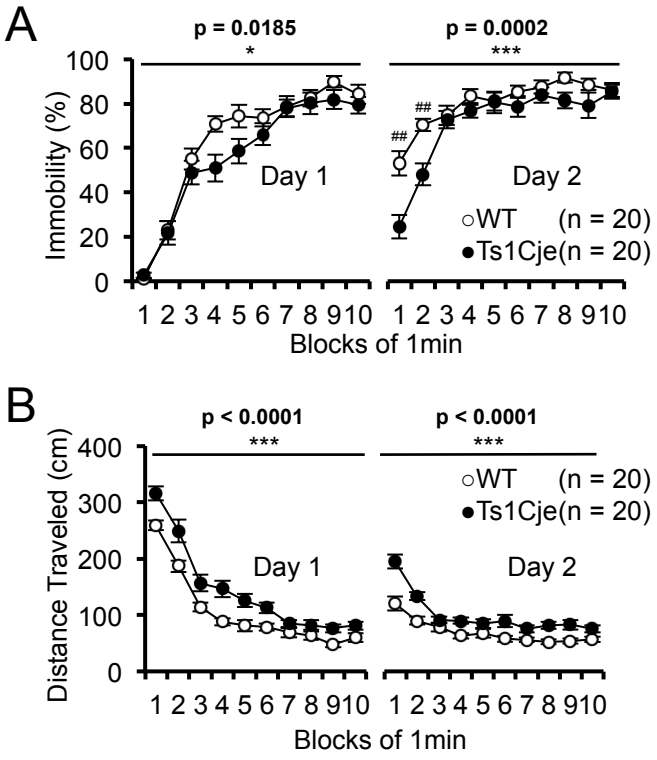

Figure 3. **Reduced depression-like behavior in Ts1Cje mice.** (A and B) In the Porsolt forced swim test, immobility time on Days 1 and 2 was significantly lower (A), whereas the distance traveled (B) was significantly higher in Ts1Cje mice when compared with WT mice at 16–18 weeks of age. P-values indicate a genotype effect in a two-way repeated-measures ANOVA (for genotype and time.) or one-way ANOVA followed by Fisher's PLSD (1 and 2 min in A, right). Data are shown as the mean (± SEM); sample numbers correspond to number of mice; * $p < 0.05$, ** $p < 0.01$, *** $p < 0.001$, and $^{\#\#}$ $p < 0.01$.

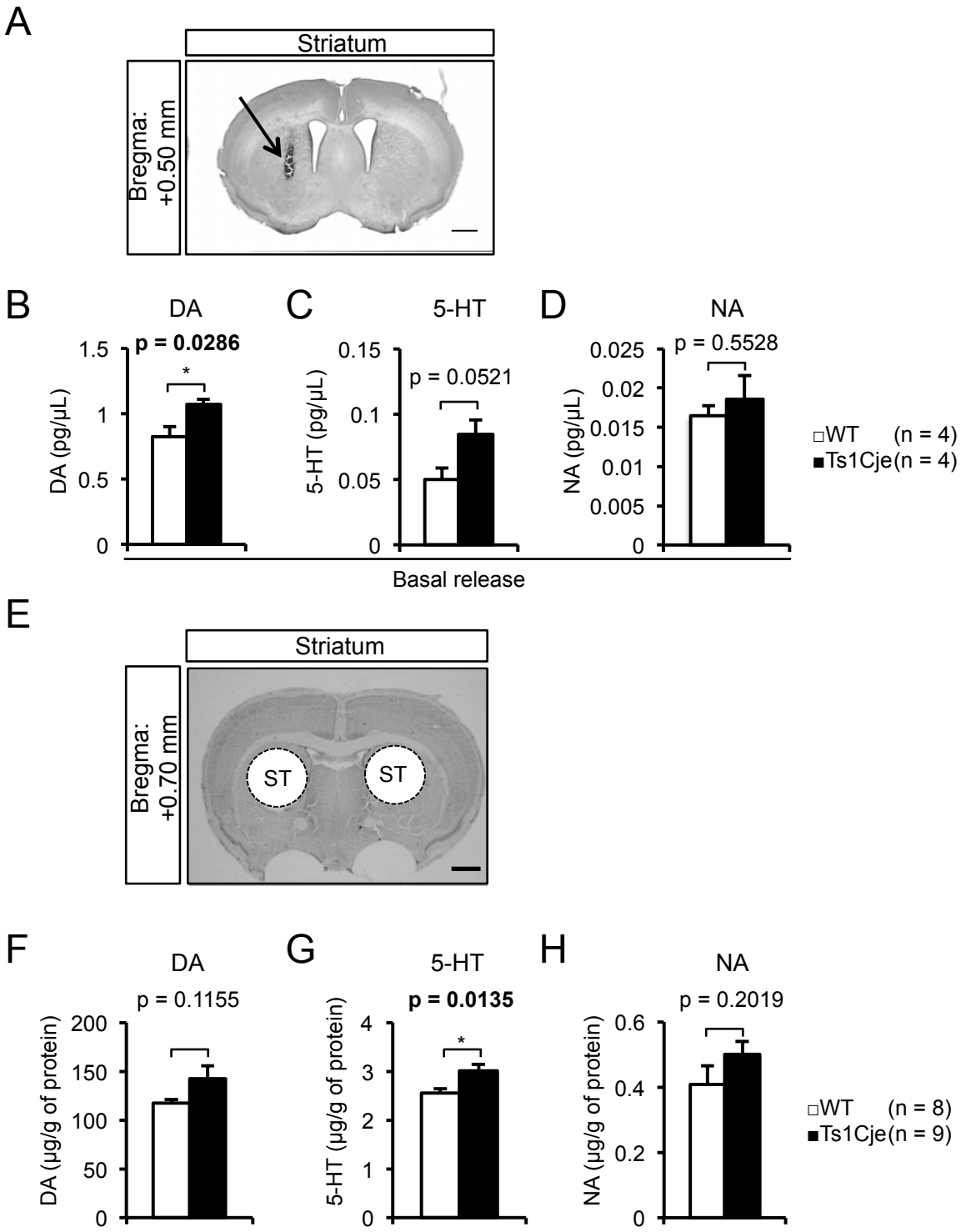

Figure 4. Increased overflow and striatal content of dopamine and serotonin in Ts1Cje mice. (A–D) Microdialysis analysis. (A) Successful targeting of microdialysis probes in the

striata of 14–16-week-old mice was confirmed by Di-I microinjection (100 μm thickness, coronal section; arrow). Overflow of DA (B), as reflected in dialysate monoamine concentrations, was significantly increased in the Ts1Cje striatum. Overflow of 5-HT (C) showed a tendency toward an increase, whereas extracellular NA levels (D) were unchanged. P-values indicate a genotype effect in a *t*-test (averaged level from repeated sampling). (E–H) Tissue-punch analysis of striatal monoamine content. (E) Representative image showing the location of excised regions for HPLC analysis from 11–14 weeks-old mice (ST: striatum). The tissue content of DA (F) and NA (H) was mildly increased in the striata of Ts1Cje mice, but this difference was not statistically significant. 5-HT content (G) was significantly higher in the Ts1Cje striatum. P-values indicate a genotype effect in a *t*-test. Data are shown as the mean (± SEM); * $p < 0.05$. Scale bars = 1 mm (A, E).

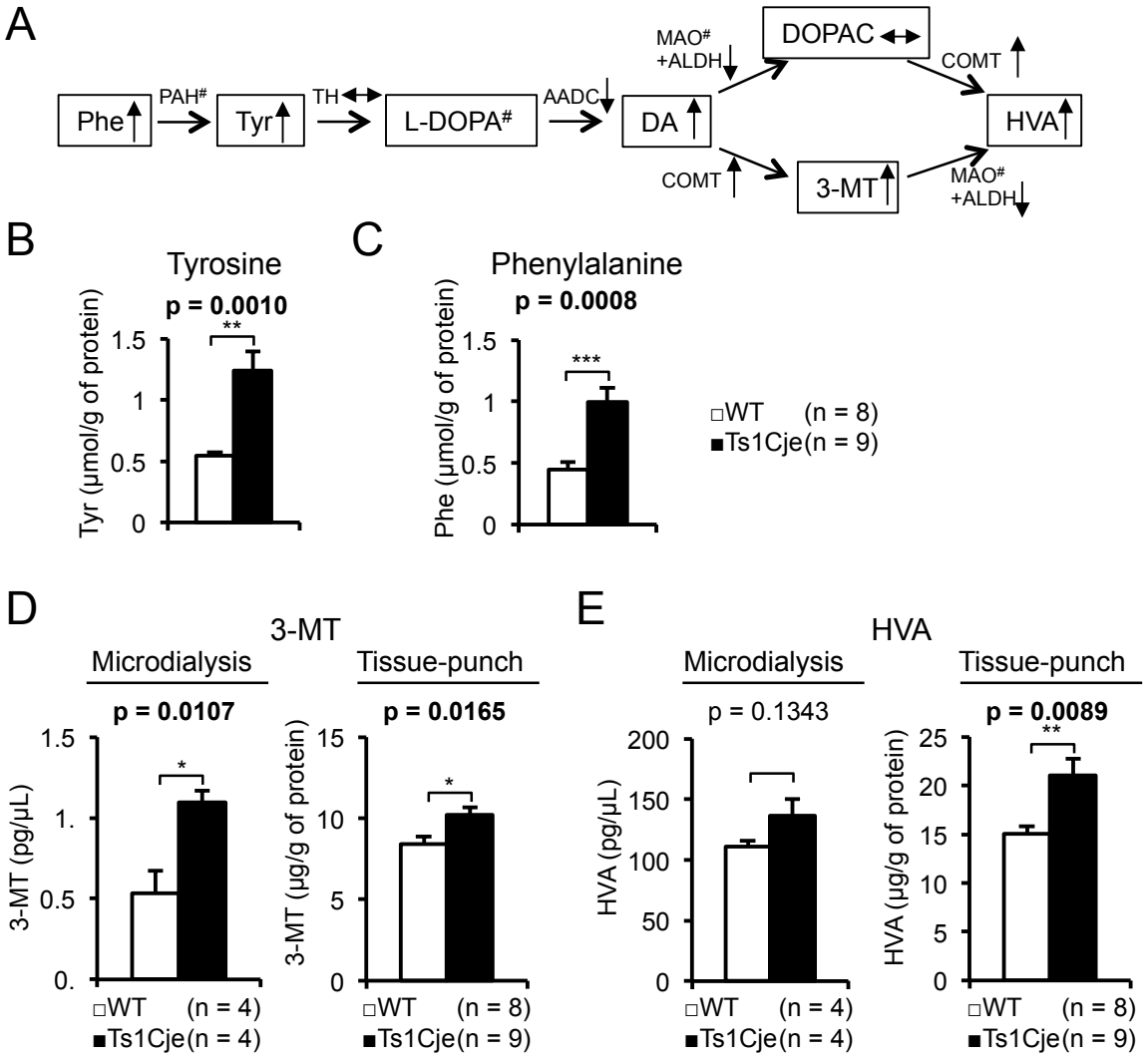

Figure 5. Increased precursors and metabolites of dopamine in Ts1Cje brain. (A) Schematic of the metabolic cascade for DA and changes in Ts1Cje mice. An increase, decrease or no change in the parameters of Ts1Cje mice are indicated by upward, downward or double horizontal arrows, respectively. # = not assessed in this study. (B, C) Amino acid content was measured in tissue extracts. Phenylalanine (Phe) and tyrosine (Tyr), which are precursors in the biosynthesis of DA, were increased in the striatum of Ts1Cje when compared with WT mice at 11–14 weeks of age. (D and E) DA metabolites. (D) 3-MT was

significantly increased in microdialysates (D, left) and tissue extracts in the Ts1Cje striatum at 11–16 weeks of age. (D, right). (E) HVA was slightly increased in striatal microdialysates (E, left) but significantly increased in striatal tissue extracts (E, right) from Ts1Cje mice at 11–16 weeks of age. P-values indicate a genotype effect in a *t*-test. Data are shown as the mean (± SEM); * $p < 0.05$, ** $p < 0.01$, and *** $p < 0.001$. PAH: phenylalanine hydroxylase, L-DOPA: L-3,4-dihydroxyphenylalanine, MAO: monoamine oxidase, Phe: phenylalanine, Tyr: tyrosine, TH: tyrosine hydroxylase, AADC: aromatic L-amino acid decarboxylase, ALDH: aldehyde dehydrogenase, COMT: catechol-*O*-methyltransferase. 3-MT: 3-methoxytyramine, DOPAC: 3, 4-dihydroxyphenylacetic acid, HVA: homovanillic acid.

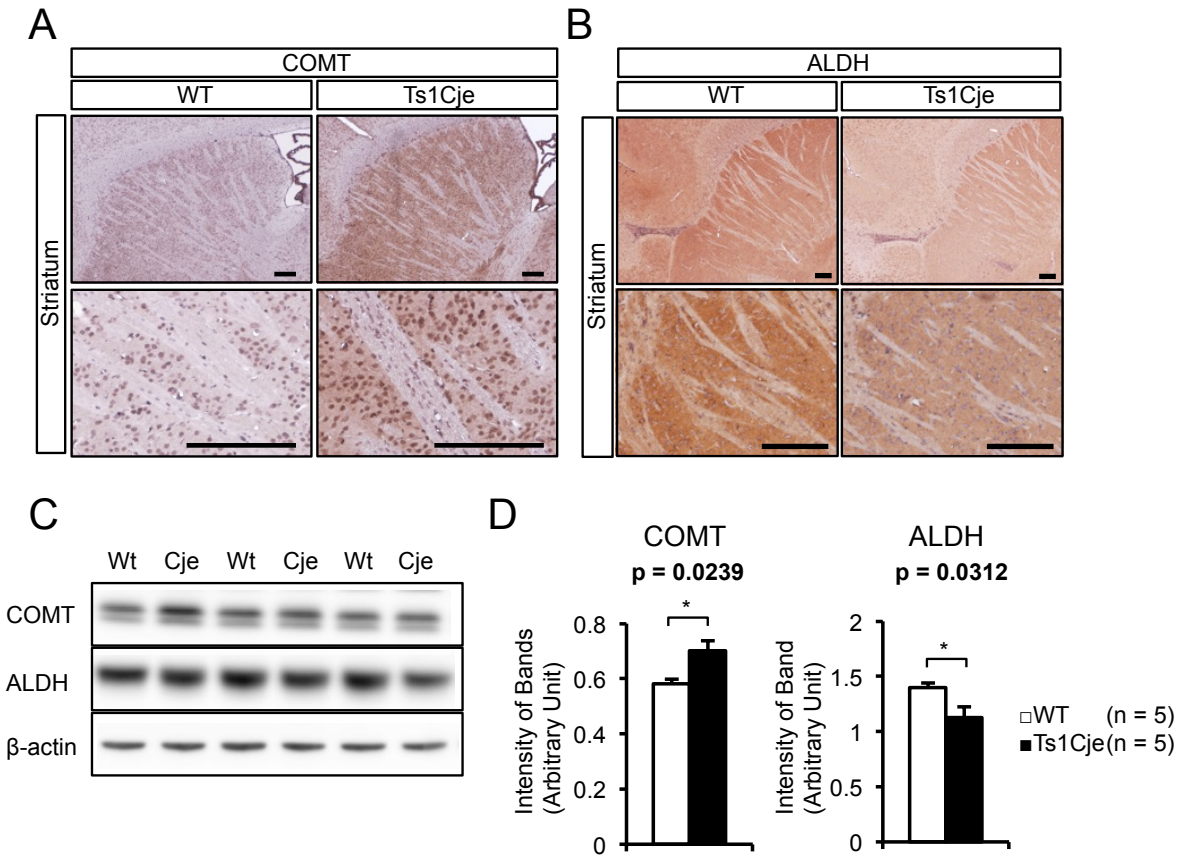

Figure 6. Increased expression of catabolic enzymes for monoamines in the striata of Ts1Cje mice. (A, B) Immunohistochemistry of catabolic enzymes for DA in the striatum. (A) The signal intensity of catechol-*O*-methyltransferase (COMT) was stronger in Ts1Cje mice at 12–15 weeks of age when compared with WT mice. (B) The signal intensity of aldehyde dehydrogenase (ALDH) tended to be lower in Ts1Cje striatum than WT striatum. Scale bars = 200 μm. (C, D) Western blot analysis of catabolic enzymes of DA in the striatum. (C) COMT and ALDH protein levels in the striatum of WT (Wt) and Ts1Cje (Cje) mice were assessed by Western blotting. β-actin was used as a loading control. (D) Quantification of band intensities revealed that the level of COMT protein was significantly increased, whereas the level of ALDH protein was significantly decreased in the striatum of Ts1Cje mice. P-values indicate a

genotype effect in a *t*-test. Data are shown as the mean (± SEM); * $p < 0.05$. COMT: catechol-*O*-methyltransferase, ALDH: aldehyde dehydrogenase.

6. Supplementary Figure

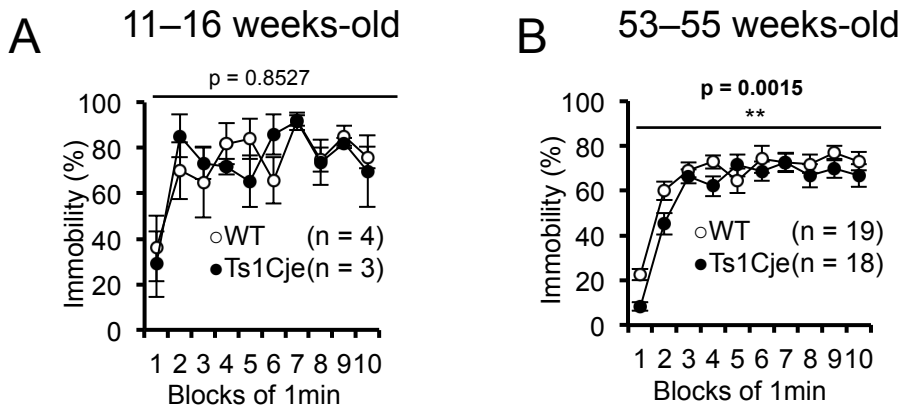

Supplementary Figure S1. **Depression-like behavior in the tail suspension test is normal in young Ts1Cje mice but significantly decreased at 1 year old.** (A and B) Tail suspension test of young adult (A) and elder mice (B). (A) No significant differences in the percentage of immobility were observed between 11–16 weeks-old WT and Ts1Cje mice. (B) The percentage of immobility was however significantly lower in 53–55 weeks-old Ts1Cje mice. P-values indicate a genotype effect in a two-way repeated-measures ANOVA. Data are shown as the mean (± SEM); * $p < 0.05$ and ** $p < 0.01$.

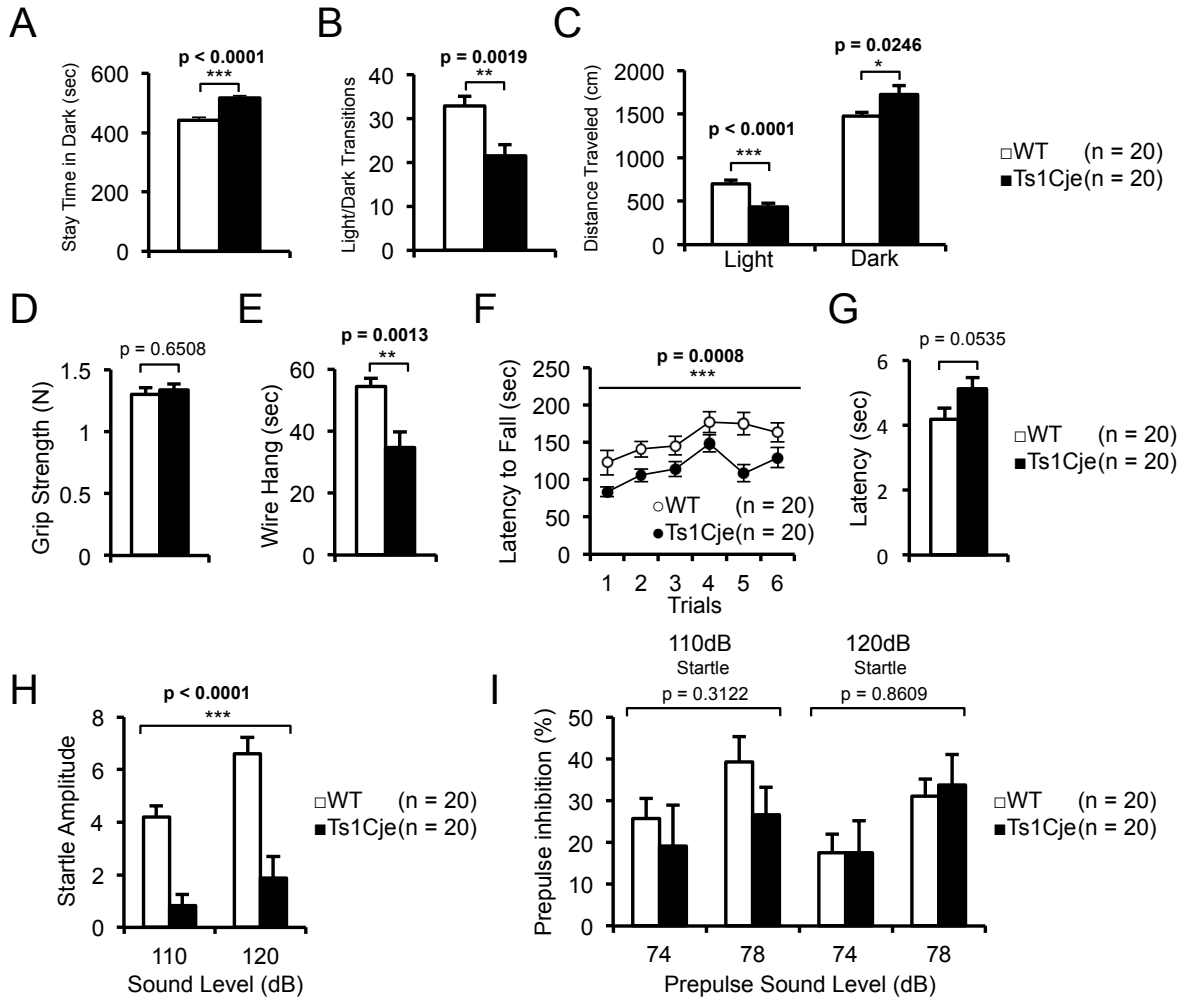

Supplementary Figure S2. Light/Dark transition, motor coordination, nociception and startle response/prepulse inhibition tests in Ts1Cje mice. (A–C) Light/dark transition test. Time spent (A) and distance traveled (C, right) in the dark compartment were significantly higher in Ts1Cje mice at 10–12 weeks of age , whereas the distance traveled in the light compartment (C, left) and number of light/dark transitions (B) were significantly lower, suggesting increased anxiety-like behavior in Ts1Cje mice in this task. (D–F) Motor function of Ts1Cje mice was assessed using grip strength, wire hang, and rotarod tests. There were no significant differences between WT and Ts1Cje mice in grip strength (D), while the latency of Ts1Cje mice to fall was significantly shorter in both the wire hang (E) and rotarod tasks (F) at

10–15 weeks of age. (G) Nociception was assessed using the hot plate test. Ts1Cje mice tended to be less sensitive than WT littermates at 12–14 weeks of age. (H, I) Startle response/prepulse inhibition (PPI) test. Ts1Cje mice displayed a significant reduction in startle amplitude (H); however, PPI was not significantly different among genotypes at 16-18 weeks of age (I). P-values indicate genotype effects in a one-way ANOVA (A–E and G) or two-way repeated-measures ANOVA (F, H and I) Data are shown as the mean (± SEM); * $p < 0.05$, ** $p < 0.01$, and *** $p < 0.001$.

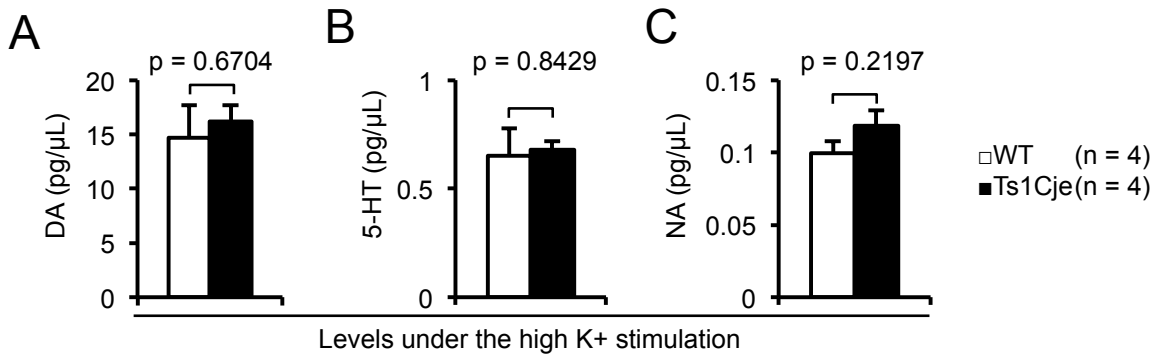

Supplementary Figure S3. Unchanged levels of extracellular monoamines in the striatum after high K^+-induced depolarization. (A–C) No significant differences in the amounts of extracellular DA, 5-HT, or NA were observed by microdialysis in the striatum of 14–16-weeks-old Ts1Cje and WT littermates with high K^+ stimulation. P-values indicate genotype effect in a *t*-test (averaged level from repeated sampling). Data are shown as the mean (± SEM).

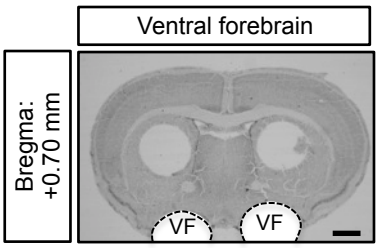

Supplementary Figure S4. Position of tissue punches taken for analysis of ventral forebrain. Representative photomicrograph showing location of punches for HPLC analyses of tissue monoamine content (VF: ventral forebrain). Scale bars = 1 mm.

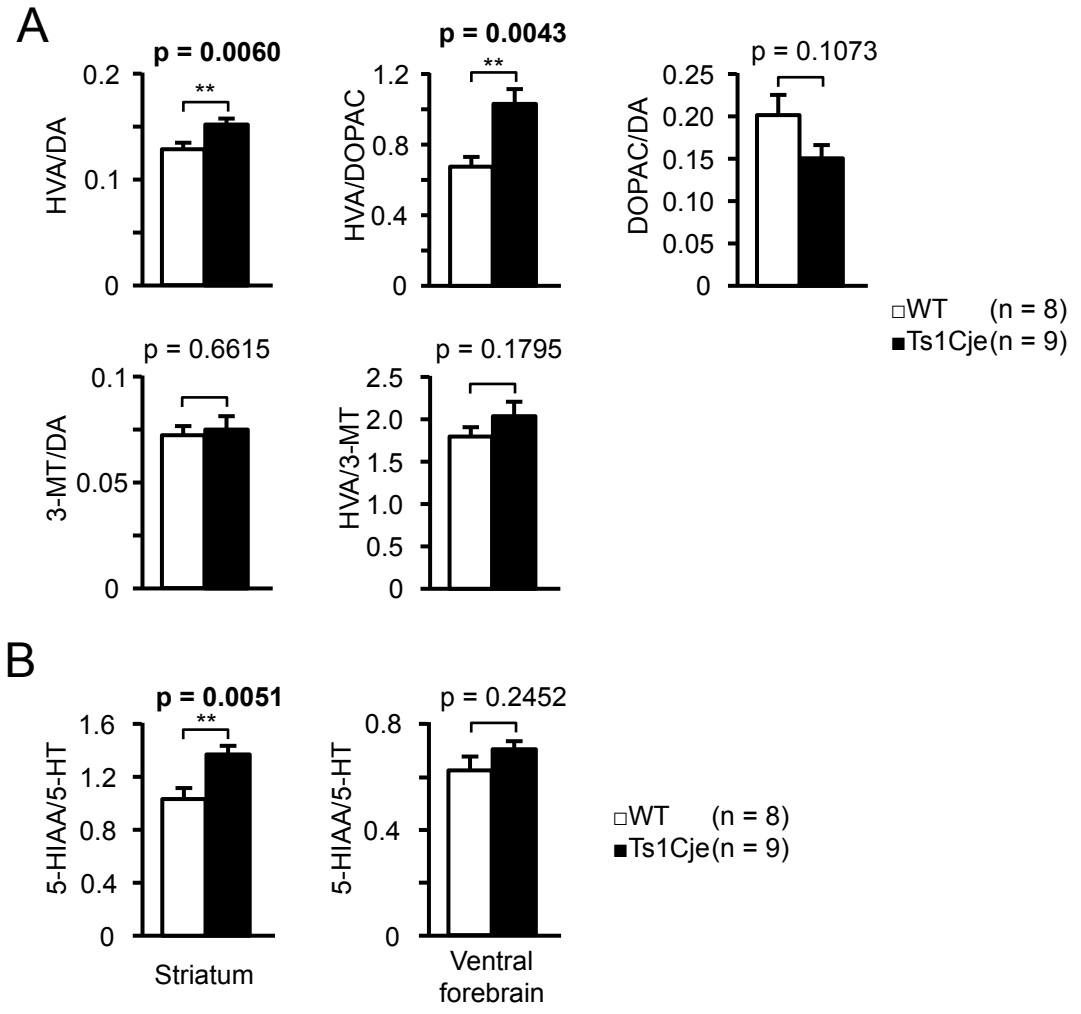

Supplementary Figure S5. Enhanced metabolism of dopamine and serotonin in 11–14-weeks-old Ts1Cje mice based on tissue extracts. (A) Disrupted turnover of DA in Ts1Cje striatum. The HVA/DA ratio in Ts1Cje striatum was increased, indicating accelerated DA catabolism (upper left). The HVA/DOPAC ratio (upper middle) was also increased, whereas the ratios for DOPAC/DA, 3-MT/DA and HVA/3-MT (upper right, lower left and lower middle) were not significantly different between WT and Ts1Cje mice (DOPAC/DA tended to be lower). (B) Disrupted turnover of 5-HT in Ts1Cje mice. The 5-HIAA/5-HT ratio was significantly increased in Ts1Cje striatum but not ventral forebrain. HVA; homovanillic acid,

DOPAC; 3,4-dihydroxyphenylacetic acid, 3-MT; 3-methoxytyramine, 5-HIAA; 5-hydroxyindoleacetic acid. P-values indicate a genotype effect in an unpaired *t*-test. Data are shown as the mean (± SEM); * $p < 0.05$ and ** $p < 0.01$.

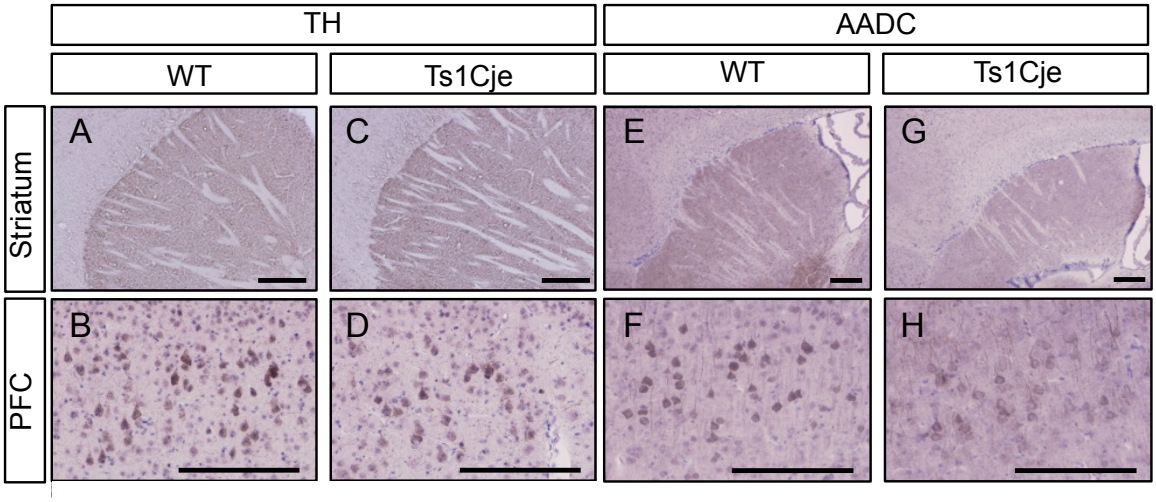

Supplementary Figure S6. Tyrosine hydroxylase (TH) and aromatic L-amino acid decarboxylase (AADC) immunohistochemical analysis in the Ts1Cje adult brain at 12–15 weeks of age. (A–D) Immunohistochemistry of TH. No obvious differences were observed in TH expression in the Ts1Cje striatum (C) or prefrontal cortex (PFC, D) compared to WT mice (A and B). (E-H) Immunohistochemistry of AADC. AADC expression levels appeared lower in the Ts1Cje striatum (G) and prefrontal cortex (H) when compared with WT littermates (E and F). Scale bars = 200 μm.

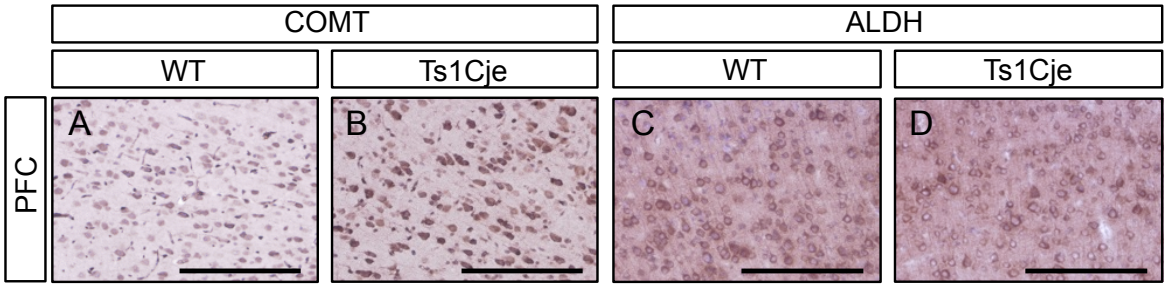

Supplementary Figure S7. Catechol-*O*-methyltransferase (COMT) and aldehyde dehydrogenase (ALDH) immunohistochemical analysis in the Ts1Cje adult brain at 12–15 weeks of age. (A, B) Immunohistochemistry of COMT. The COMT signal intensity was stronger in the Ts1Cje prefrontal cortex (PFC) when compared with the WT. (C, D) Immunohistochemistry of ALDH. ALDH expression tended to be lower in Ts1Cje brains when compared with the corresponding WT brain regions. Scale bars = 200 μm.

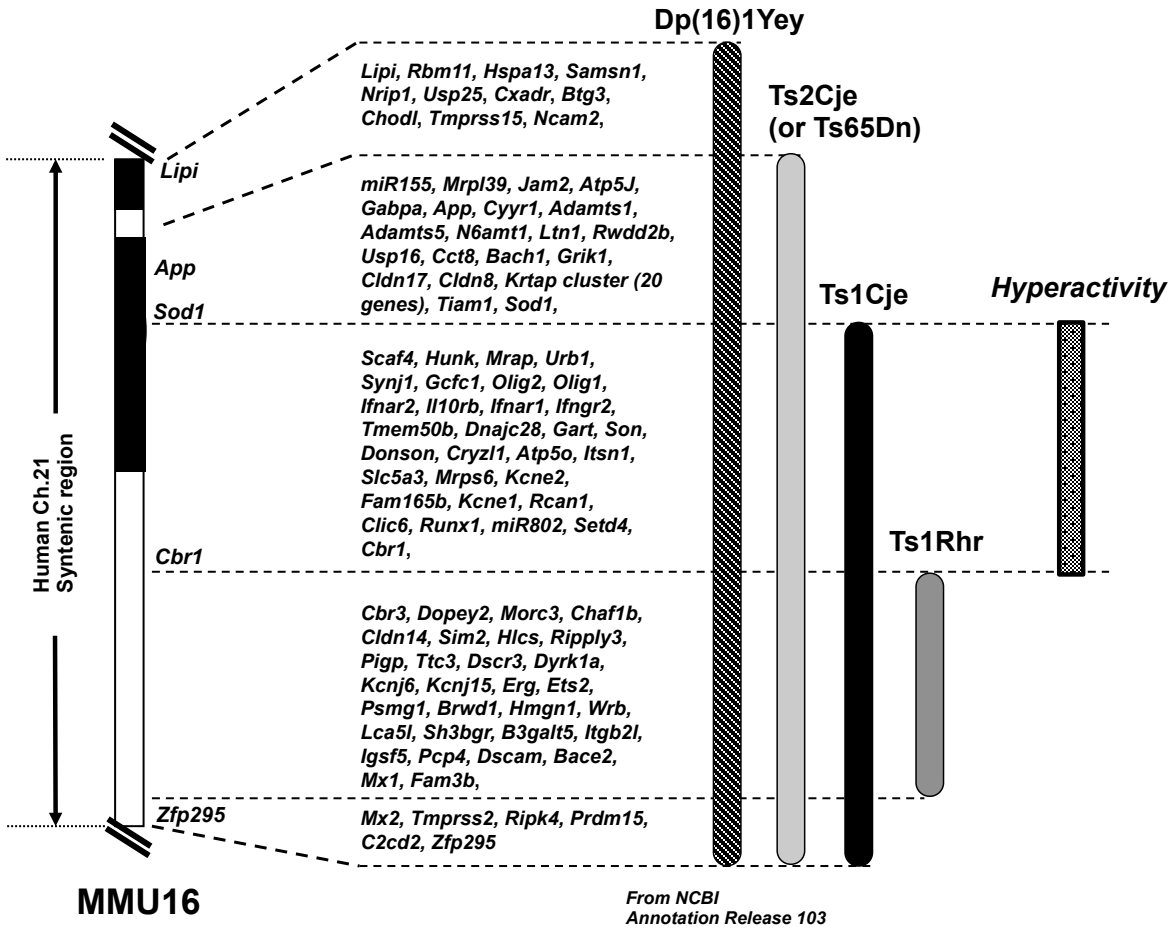

Supplementary Figure S8. Genes on the trisomic segments of Down syndrome model mice. Some of the genes responsible for the hyperactivity phenotype are likely located within the Ts1Cje specific trisomic region.

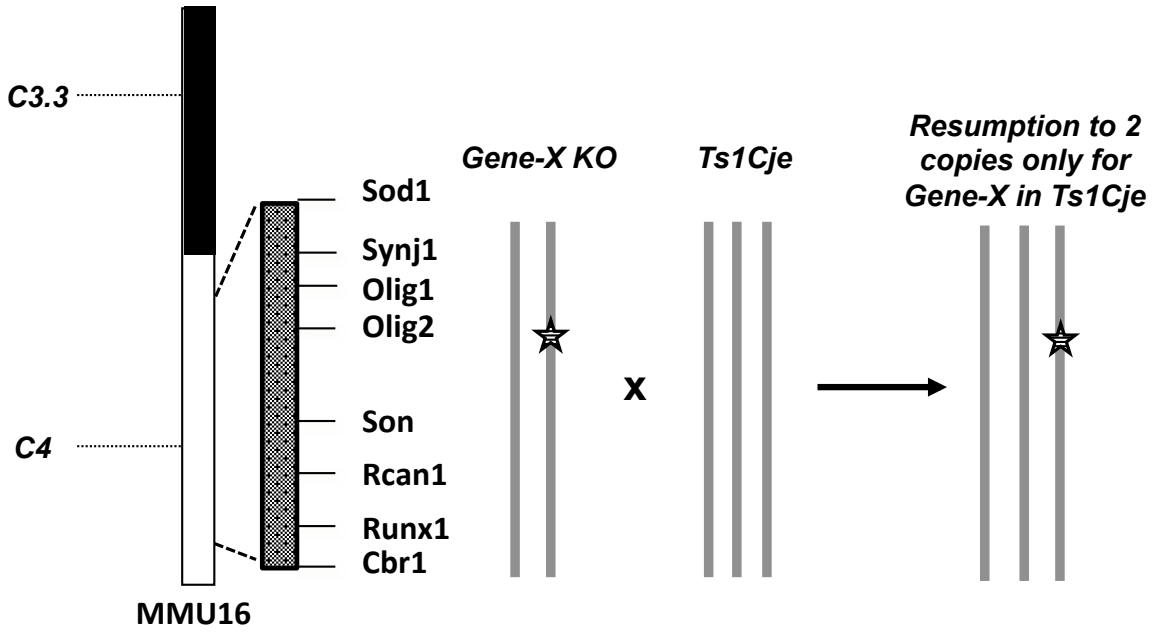

Supplementary Figure S9. Schematic diagram for subtractive approach to evaluate a candidate gene. Down syndrome model mouse with partial trisomy is mated with "Gene-X" knockout mouse. In the resulting compound mouse, the copy number of the candidate gene is resumed to two copies while other genes on the trisomic segments remain in three copies.

7. Table

Table 1. Comprehensive behavioral test battery of Ts1Cje mice

	Behavior task	Age (w)
Batch 1	1. General health and Neurological screen	10-12
	2. Grip Strength / Wire hanging	10-12
	3. Light/dark transition	10-12
	4. Open field	10-13
	5. Elevated plus maze	11-13
	6. Hot plate	12-14
	7. Social interaction (novel environment)	12-14
	8. Rotarod	12-15
	9. Social interaction (three chamber)	13-16
	10. Startle response/PPI	16-18
	11. Porsolt forced swim	16-18
	12. Tail suspension	53-55
Batch 2	24 hours home cage activity monitoring	12-13
Batch 3	Tail suspension	11-16

Age (w): age in weeks at the beginning of the test

Table 2. Monoamine content and overflow in Ts1Cje brain.

		Microdialysis		
		WT (n = 4)	Ts1Cje (n = 4)	*P* values (WT vs Ts1Cje)
Striatum	DA	0.823 ± 0.077	1.072 ± 0.040	* **0.0286**
	5-HT	0.050 ± 0.008	0.084 ± 0.011	0.0521
	NA	0.016 ± 0.001	0.019 ± 0.003	0.5528
		Tissue-punch		
		WT (n = 8)	Ts1Cje (n = 9)	*P* values (WT vs Ts1Cje)
Striatum	DA	117639.5 ± 3557	142287.5 ± 13498.7	0.1155
	5-HT	2554.0 ± 83.6	3007.8 ± 133.2	* **0.0135**
	NA	408.6 ± 56.7	499.5 ± 39.9	0.2019
Ventral forebrain	DA	40355.8 ± 3807.0	48368.3 ± 5392.0	0.2545
	5-HT	6185.7 ± 306.3	8030.2 ± 460.3	** **0.0054**
	NA	1770.7 ± 263.1	2592.4 ± 243.6	* **0.0366**

Microdialysis: Results are given in pg/µL; Tissue punch: Results are given in ng/g of protein; each value represents the mean ± SEM. Mouse age: 3-month.
* $p < 0.05$, ** $p < 0.01$, Abbreviation; DA: dopamine, 5-HT: serotonin, NA: noradrenaline

Table 3. Contents of amino acids in Ts1Cje brain

		WT (n = 8)	Ts1Cje (n = 9)	*P* values (WT vs Ts1Cje)
Striatum	Ala	4.36 ± 0.28	5.67 ± 0.70	0.1196
	Asp	14.19 ± 0.94	17.92 ± 2.75	0.2427
	Glu	67.88 ± 4.03	87.09 ± 10.98	0.1390
	Gly	7.04 ± 0.43	9.48 ± 1.14	0.0769
	Phe	0.45 ± 0.06	1.00 ± 0.11	*** **0.0008**
	Ser	6.49 ± 0.40	7.63 ± 0.82	0.2518
	Tyr	0.54 ± 0.03	1.24 ± 0.16	** **0.0010**
Ventral forebrain	Ala	4.41 ± 0.31	5.32 ± 0.60	0.2091
	Asp	19.68 ± 0.89	25.11 ± 2.67	0.0861
	Glu	61.11 ± 5.21	76.66 ± 10.42	0.2192
	Gly	6.34 ± 0.25	8.86 ± 0.74	** **0.0082**
	Phe	0.25 ± 0.04	0.78 ± 0.19	* **0.0192**
	Ser	4.72 ± 0.22	5.68 ± 0.60	0.1709
	Tyr	0.41 ± 0.06	1.12 ± 0.25	* **0.0206**

Results are given in µmol/g of protein; each value represents the mean ± SEM. Mouse age: 3 month, * $p < 0.05$, ** $p < 0.01$, *** $p < 0.001$, Abbreviation; Ala: alanine, Asp: aspartate, Glu: glutamate, Gly: glycine, Phe: phenylalanine, Ser: serine, Tyr: tyrosine

Table 4. Monoamine metabolite content in Ts1Cje brain.

		Microdialysis		
		WT (n = 4)	Ts1Cje (n = 4)	*P* values (WT vs Ts1Cje)
Striatum	DOPAC	173.463 ± 10.062	168.023 ± 20.647	0.8206
	3-MT	0.535 ± 0.137	1.097 ± 0.071	* **0.0107**
	HVA	111.370 ± 4.667	136.488 ± 13.745	0.1343
	5-HIAA	39.925 ± 2.673	61.241 ± 6.747	* **0.0260**
		Tissue-punch		
		WT (n = 8)	Ts1Cje (n = 9)	*P* values (WT vs Ts1Cje)
Striatum	DOPAC	24352.0 ± 3501.6	21293.7 ± 2145.8	0.4568
	3-MT	8421.1 ± 456.7	10191.5 ± 466.3	* **0.0165**
	HVA	15081.0 ± 731.2	21024.6 ± 1744.7	** **0.0089**
	5-HIAA	2650.5 ± 184.7	4114.2 ± 310.8	** **0.0014**
Ventral forebrain	DOPAC	16122.4 ± 3058.0	15118.2 ± 1714.6	0.7719
	3-MT	4684.8 ± 632.1	4952.1 ± 533.5	0.7493
	HVA	7305.3 ± 962.6	9442.4 ± 920.1	0.1297
	5-HIAA	3954.8 ± 577.0	5642.7 ± 379.9	* **0.0247**

Microdialysis: Results are given in pg/μL; Tissue punch: Results are given in ng/g of protein; each value represents the mean ± SEM.
Mouse age: 3-month, * $p < 0.05$, ** $p < 0.01$, Abbreviation; DOPAC: 3, 4-dihydroxyphenylacetic acid, 3-MT: 3-methoxytyramine, HVA: homovanillic acid, 5-HIAA: 5-hydroxyindoleacetic acid

8. Acknowledgments

I would like to thank Dr. Kazuhiro Yamakawa for giving me an opportunity to do my PhD work in his lab, for his great supervision, and for evaluation of my work. I would like to thank Dr. Keiichi Ishihara, Dr. Hiroyuki Miyamoto, Dr. Matthieu Raveau, Dr. Abdul Shukkur Ebrahim, Dr. Hiroko Omi and Dr. Kenji Amano at Neurogenetics Lab. for their support to characterize the phenotypes of DS model mice. I would like to thank Dr. Satoko Hattori and Dr. Tsuyoshi Miyakawa for behavioral analyses. I would like to thank Dr. Hiromasa Morishita and Dr. Nobuko Mataga for *in vivo* microdialysis of Ts1Cje mice. I would like to thank Dr. Guy Ornthanalai and Dr. Niall P. Murphy for biological analyses of Ts1Cje mice. I would like to thank Dr. Kazuyuki Yamada for his help with behavioral testing. I would like to thank Dr. Haruhiko Sago for providing me with Ts1Cje mice. I would like to thank Dr. Satoshi Akiba and Ms. Lisa Beppu for completing the immunohistochemistry. I also would like to thank all my collaborators, my past and present lab members; Dr. Toshimitsu Suzuki, Dr. Tetsuya Tatsukawa, Dr. Tetsushi Yamagata, Dr. Genki Sudo, Mrs. Emi Mazaki, Dr. Ikuo Ogiwara, Mrs. Miyuki Murayama and Ms. Ikuyo Inoue for their enormous support. I am indebted to the Research Resources Center of the RIKEN Brain Science Institute for animal care and help with the behavioral analysis.

9. References

Amano, K., Sago, H., Uchikawa, C., Suzuki, T., Kotliarova, S.E., Nukina, N., Epstein, C.J., Yamakawa, K., 2004. Dosage-dependent over-expression of genes in the trisomic region of Ts1Cje mouse model for Down syndrome. Hum. Mol. Genet. 13, 333-340.

Belichenko, P.V., Kleschevnikov, A.M., Salehi, A., Epstein, C.J., Mobley, W.C., 2007. Synaptic and cognitive abnormalities in mouse models of Down syndrome: exploring genotype-phenotype relationships. J. Comp. Neurol. 504, 329-345.

Belichenko, N.P., Belichenko, P.V., Kleschevnikov, A.M., Salehi, A., Reeves, R.H., Mobley, W.C. 2009. The "Down syndrome critical region" is sufficient in the mouse model to confer behavioral, neurophysiological, and synaptic phenotypes characteristic of Down syndrome. J. Neurosci. 29, 5938-5948.

Brahe, C., Serra, A., Morton, N.E., 1985. Erythrocyte catechol-O-methyltransferase activity: genetic analysis in nuclear families with one child affected by Down syndrome. Am. J. Med. Genet. 21, 373-384.

Collacott, R.A., Cooper, S.A., McGrother, C., 1992. Differential rates of psychiatric disorders in adults with Down's syndrome compared with other mentally handicapped adults. Br. J. Psychiatry. 161, 671-674.

Coussons-Read, M.E., Crnic, L.S., 1996. Behavioral assessment of the Ts65Dn mouse, a model for Down syndrome: Altered behavior in the elevated plus maze and open field. Behav. Genet. 26, 7-13.

Crawley, J.N., 2004. Designing mouse behavioral tasks relevant to autistic-like behaviors. Ment. Retard. Dev. Disabil. Res. Rev. 10, 248-258.

Das, I., Reeves, R.H., 2011. The use of mouse models to understand and improve cognitive

deficits in Down syndrome. Dis. Model. Mech. 4, 596-606.

Davisson, M.T., Schmidt, C., Akeson, E.C., 1990. Segmental trisomy of murine chromosome 16: a new model system for studying Down syndrome. Prog. Clin. Biol. Res. 360:263-280.

Duchon, A., Raveau, M., Chevalier, C., Nalesso, V., Sharp, A.J., Herault, Y., 2011. Identification of the translocation breakpoints in the Ts65Dn and Ts1Cje mouse lines: relevance for modeling Down syndrome. Mamm. Genome. 22, 674-684.

Epstein, C.J., 2001. Down syndrome (trisomy 21), in: Scriver, C.R., Beaudet, A.L., Sly, W.S., Valle, D. (Eds.), The Metabolic and Molecular Bases Inherited Disease. 8th edition. New York: McGraw Hill. p. 1223-1256.

Fernandez, F., Garner, C.C., 2007. Object recognition memory is conserved in Ts1Cje, a mouse model of Down syndrome. Neurosci. Lett. 421, 137-141.

Fernandez, F., Morishita, W., Zuniga, E., Nguyen, J., Blank, M., Malenka, R.C., Garner, C.C., 2007. Pharmacotherapy for cognitive impairment in a mouse model of Down syndrome. Nat. Neurosci. 10, 411-413.

Gibbs, M.V., Thorpe, J.G., 1983. Personality stereotype of noninstitutionalized Down syndrome children. Am. J. Ment. Defic. 87, 601-605.

Giros, B., Jaber, M., Jones, S.R., Wightman, R.M., Caron, M.G., 1996. Hyperlocomotion and indifference to cocaine and amphetamine in mice lacking the dopamine transporter. Nature. 379, 606-612.

Godridge, H., Reynolds, G.P., Czudek, C., Calcutt, N.A., Benton, M., 1987. Alzheimer-like neurotransmitter deficits in adult Down's syndrome brain tissue. J. Neurol. Neurosurg. Psychiatry. 50, 775-778.

Gordon, J.A., Hen, R., 2004. Genetic approaches to the study of anxiety. Annu. Rev. Neurosci. 27, 193-222.

Guedj, F., Pennings, J.L., Wick, H.C., Bianchi, D.W., 2015. Analysis of adult cerebral cortex and hippocampus transcriptomes reveals unique molecular changes in the Ts1Cje mouse model of down syndrome. Brain Pathol. 25, 11-23.

Gustavson, K.H., Flodérus, Y., Jagell, S., Wetterberg, L., Ross, S.B., 1982. Catechol-o-methyltransferase activity in erythrocytes in Down's syndrome: family studies. Clin. Genet. 22, 22-24.

Gustavson, K.H., Wetterberg, L., Bäckström, M., Ross, S.B., 1973. Catechol-O-methyltransferase activity in erythrocytes in Down's syndrome. Clin. Genet. 4, 279-280.

Hattori, S., Takao, K., Tanda, K., Toyama, K., Shintani, N., Baba, A., Hashimoto, H., Miyakawa, T., 2012. Comprehensive behavioral analysis of pituitary adenylate cyclase-activating polypeptide (PACAP) knockout mice. Front. Behav. Neurosci. 6, 58.

Heller, H.C., Salehi, A., Chuluun, B., Das, D., Lin, B., Moghadam, S., Garner, C.C., Colas, D., 2014. Nest building is impaired in the Ts65Dn mouse model of Down syndrome and rescued by blocking 5HT2a receptors. Neurobiol. Learn Mem. 116, 162-171.

Holmes, A., Parmigiani, S., Ferrari, P.F., Palanza, P., Rodgers, R.J., 2000. Behavioral profile of wild mice in the elevated plus-maze test for anxiety. Physiol. Behav. 71, 509-516.

Hovatta, I., Barlow, C., 2008. Molecular genetics of anxiety in mice and men. Ann. Med. 40, 92-109.

Ishihara, K., Amano, K., Takaki, E., Ebrahim, A.S., Shimohata, A., Shibazaki, N., Inoue, I., Takaki, M., Ueda, Y., Sago, H., Epstein, C.J., Yamakawa, K., 2009. Increased lipid peroxidation in Down's syndrome mouse models. J. Neurochem. 110, 1965-1976.

Ishihara, K., Amano, K., Takaki, E., Shimohata, A., Sago, H., Epstein, C.J., Yamakawa K., 2010. Enlarged brain ventricles and impaired neurogenesis in the Ts1Cje and Ts2Cje mouse models of Down syndrome. Cereb. Cortex. 20, 1131-1143.

Ishihara, K., Kanai, S., Sago, H., Yamakawa, K., Akiba, S., 2014. Comparative proteomic profiling reveals aberrant cell proliferation in the brain of embryonic Ts1Cje, a mouse model of Down syndrome. Neuroscience. 28, 1-15.

Kasari, C., Mundy, P., Yirmiya, N., Sigman, M., 1990. Affect and attention in children with Down syndrome. Am. J. Ment. Retard. 95, 55-67.

Kleschevnikov, A.M., Belichenko, P.V., Faizi, M., Jacobs, L.F., Htun, K., Shamloo, M., Mobley, W.C., 2012. Deficits in cognition and synaptic plasticity in a mouse model of Down syndrome ameliorated by GABAB receptor antagonists. J. Neurosci. 32, 9217-9227.

Kay, A.D., Schapiro, M.B., Riker, A.K., Haxby, J.V., Rapoport, S.I., Cutler, N.R., 1987. Cerebrospinal fluid monoaminergic metabolites are elevated in adults with Down's syndrome. Ann. Neurol. 21, 408-411.

Komada, M., Takao, K., Miyakawa, T. 2008. Elevated plus maze for mice. J. Vis. Exp. 22, e1088.

Lubec, G., Labudova, O., Cairns, N., Berndt, P., Langen, H., Fountoulakis, M., 1999. Reduced aldehyde dehydrogenase levels in the brain of patients with Down syndrome. J. Neural. Transm. Suppl. 57, 21-40.

Mann, D.M., Yates, P.O., Marcyniuk, B., Ravindra, C.R., 1985. Pathological evidence for neurotransmitter deficits in Down's syndrome of middle age. J. Ment. Defic. Res. 29, 125-135.

Mantry, D., Cooper, S.A., Smiley, E., Morrison, J., Allan, L., Williamson, A., Finlayson, J., Jackson, A., 2008. The prevalence and incidence of mental ill-health in adults with Down syndrome. J Intellect. Disabil. Res. 52, 141-155.

McCall, J.G., Al-Hasani, R., Siuda, E.R., Hong, D.Y., Norris, A.J., Ford, C.P., Bruchas, M.R., 2015. CRH Engagement of the Locus Coeruleus Noradrenergic System Mediates Stress-Induced Anxiety. Neuron. 87, 605-620.

McCarthy, J., Boyd, J., 2001. Psychopathology and young people with Down's syndrome: childhood predictors and adult outcome of disorder. J. Intellect. Disabil. Res. 45, 99-105.

Mefford, I.N., 1981. Application of high performance liquid chromatography with electrochemical detection to neurochemical analysis: measurement of catecholamines, serotonin and metabolites in rat brain. J. Neurosci. Methods. 3, 207-224

Megías. M., Verduga, R., Dierssen, M., Flórez, J., Insausti, R., Crespo, D., 1997. Cholinergic, serotonergic and catecholaminergic neurons are not affected in Ts65Dn mice. Neuroreport. 8, 3475-3478.

Mosienko, V., Bert, B., Beis, D., Matthes, S., Fink, H., Bader, M., Alenina, N., 2012. Exaggerated aggression and decreased anxiety in mice deficient in brain serotonin. Transl. Psychiatry. 2, e122.

Moy, S.S., Nadler, J.J., Perez, A., Barbaro, R.P., Johns, J.M., Magnuson, T.R., Piven, J., Crawley, J.N., 2004. Sociability and preference for social novelty in five inbred strains: an approach to assess autistic-like behavior in mice. Genes Brain Behav. 3, 287-302.

Nakao, A., Miki, T., Shoji, H., Nishi, M., Takeshima, H., Miyakawa, T., Mori, Y., 2015. Comprehensive behavioral analysis of voltage-gated calcium channel beta-anchoring and -regulatory protein knockout mice. Front. Behav. Neurosci. 9, 141

Nygaard, E., Smith, L., Torgersen, A.M., 2002. Temperament in children with Down syndrome and in prematurely born children. Scand. J. Psychol. 43, 61-71.

Olson, L.E., Roper, R.J., Sengstaken, C.L., Peterson, E.A., Aquino, V., Galdzicki, Z., Siarey, R., Pletnikov, M., Moran, T.H., Reeves, R.H., 2007. Trisomy for the Down syndrome 'critical region' is necessary but not sufficient for brain phenotypes of trisomic mice. Hum. Mol. Genet. 16, 774-782.

Paxinos, G., Franklin, K.B.J., 2001. The Mouse Brain in Stereotaxic Coordinates, Second edition. San Diego: Academic Press.

Pueschel, S.M., Bernier, J.C., Pezzullo, J.C., 1991. Behavioural observations in children with Down's syndrome. J. Ment. Defic. Res. 35, 502-511.

Raveau, M., Nakahari, T., Asada, S., Ishihara, K., Amano, K., Shimohata, A., Sago, H., Yamakawa, K., 2017. Brain ventriculomegaly in Down syndrome mice is caused by Pcp4 dose-dependent cilia dysfunction. Hum. Mol. Genet. 26, 923-931.

Reeves, R.H., Irving, N.G., Moran, T.H., Wohn, A., Kitt, C., Sisodia, S.S., Schmidt, C., Bronson, R.T., Davisson, M.T., 1995. A mouse model for Down syndrome exhibits learning and behaviour deficits. Nat. Genet. 11, 177-184.

Reynolds, G.P., Godridge, H., 1985. Alzheimer-like brain monoamine deficits in adults with Down's syndrome. Lancet. 2, 1368-1369.

Richtsmeier, J.T., Baxter L.L., Reeves, R.H., 2000. Parallels of craniofacial maldevelopment in Down syndrome and Ts65Dn mice. Dev. Dyn. 217, 137-145.

Richtsmeier, J.T., Zumwalt, A., Carlson, E.J., Epstein, C.J., Reeves, R.H., 2002. Craniofacial phenotypes in segmentally trisomic mouse models for Down syndrome. Am. J. Med. Genet. 107, 317-324.

Risser, D., Lubec, G., Cairns, N., Herrera-Marschitz, M., 1997. Excitatory amino acids and monoamines in parahippocampal gyrus and frontal cortical pole of adults with Down syndrome. Life Sci. 60, 1231-1237.

Roeper, J., 2013. Dissecting the diversity of midbrain dopamine neurons. Trends Neurosci. 36, 336-342.

Rowley, H.L., Martin, K.F., Marsden, C.A., 1995. Determination of in vivo amino acid neurotransmitters by high-performance liquid chromatography with o-phthalaldehyde-sulphite derivatisation. J. Neurosci. Methods. 57, 93-99.

Sago, H., Carlson, E.J., Smith, D.J., Kilbridge, J., Rubin, E.M., Mobley, W.C., Epstein, C.J., Huang, T.T., 1998. Ts1Cje, a partial trisomy 16 mousemodel for Downsyndrome, exhibits learning and behavioral abnormalities. Proc. Natl. Acad. Sci. U.S.A. 95, 6256–6261.

Sago, H., Carlson, E.J., Smith, D.J., Rubin, E.M., Crnic, L.S., Huang, T.T., Epstein, C.J., 2000. Genetic dissection of region associated with behavioral abnormalities in mouse models for Down syndrome. Pediatr. Res. 48, 606-613.

Salehi, A., Faizi, M., Colas, D., Valletta, J., Laguna, J., Takimoto-Kimura, R., Kleschevnikov, A., Wagner, S.L., Aisen, P., Shamloo, M., Mobley, W.C., 2009. Restoration of norepinephrine-modulated contextual memory in a mouse model of Down syndrome. Sci. Transl. Med. 1, 7ra17.

Schapiro, M.B., Kay, A.D., May, C., Ryker, A.K., Haxby, J.V., Kaufman, S., Milstien, S., Rapoport, S.I., 1987. Cerebrospinal fluid monoamines in Down's syndrome adults at different ages. J. Ment. Defic. Res. 31, 259-269.

Seidl, R., Kaehler, S.T., Prast, H., Singewald, N., Cairns, N., Gratzer, M., Lubec, G., 1999.

Serotonin (5-HT) in brains of adult patients with Down syndrome. J. Neural. Transm. Suppl. 57, 221-232.

Shichiri, M., Yoshida, Y., Ishida, N., Hagihara, Y., Iwahashi, H., Tamai, H., Niki, E., 2011. α-Tocopherol suppresses lipid peroxidation and behavioral and cognitive impairments in the Ts65Dn mouse model of Down syndrome. Free Radic. Biol. Med. 50, 1801-1811.

Shimohata, A., Ishihara, K., Hattori, S., Miyamoto, H., Morishita, H., Ornthanalai, G., Raveau, M., Ebrahim, A.S., Amano, K., Yamada, K., Sago, H., Akiba, S., Mataga, N., Murphy, N.P., Miyakawa, T., Yamakawa, K., 2017. Ts1Cje Down syndrome model mice exhibit environmental stimuli-triggerd locomotor hyperactivity and sociability concurrent with increased flux through central dopamine and serotonin metabolism. Exp. Neurol. 293, 1-12.

Shukkur, E.A, Shimohata, A., Akagi, T., Yu, W., Yamaguchi, M., Murayama, M., Chui, D., Takeuchi, T., Amano, K., Subramhanya, K.H., Hashikawa, T., Sago, H., Epstein, C.J., Takashima, A., Yamakawa, K., 2006. Mitochondrial dysfunction and tau hyperphosphorylation in Ts1Cje, a mouse model for Down syndrome. Hum. Mol. Genet. 15, 2752-2762.

Siarey, R.J., Villar, A.J., Epstein, C.J., Galdzicki, Z., 2005. Abnormal synaptic plasticity in the Ts1Cje segmental trisomy 16 mouse model of Down syndrome. Neuropharmacology. 49, 122-128.

Stein, D.S., Munir, K.M., Karweck, A.J., Davidson, E.J., Stein, M.T., 2013. Developmental regression, depression, and psychosocial stress in an adolescent with Down syndrome. J. Dev. Behav. Pediatr. 34, 216-218.

Takao K, Miyakawa T (2006) Light/dark transition test for mice. J Vis Exp 1:e104.

Tse, W.S., Bond, A.J., 2002. Serotonergic intervention affects both social dominance and affiliative behaviour. Psychopharmacology. 161, 324-330.

Villar, A.J., Belichenko, P.V., Gillespie, A.M., Kozy, H.M., Mobley, W.C., Epstein, C.J., 2005. Identification and characterization of a new Down syndrome model, Ts[Rb(12.1716)]2Cje, resulting from a spontaneous Robertsonian fusion between T(1716)65Dn and mouse chromosome 12. Mamm. Genome. 16, 79-90.

Walker, J.C., Dosen, A., Buitelaar, J.K., Janzing, J.G., 2011. Depression in Down syndrome: a review of the literature. Res. Dev. Disabil. 32, 1432-1440.

Wood, P.L., Nair, N.P., Bozarth, M., 1982. Striatal 3-methoxytyramine as an index of dopamine release effects of electrical stimulation. Neurosci. Lett. 32, 291-294.

Xu, F., Gainetdinov, R.R., Wetsel, W.C., Jones, S.R., Bohn, L.M., Miller, G.W., Wang, Y.M., Caron, M.G., 2000. Mice lacking the norepinephrine transporter are supersensitive to psychostimulants. Nat. Neurosci. 3, 465-471.

Yates, C.M., Simpson, J., Gordon, A., Maloney, A.F., Allison, Y., Ritchie, I.M., Urquhart, A., 1983. Catecholamines and cholinergic enzymes in pre-senile and senile Alzheimer-type dementia and Down's syndrome. Brain Res. 280, 119-126.